

Kumaraswamy Alpha Power Lomax Distribution: Properties and Applications in Actuarial Sciences

Wondimu Fikre ^{1,2,*}, Harmanpreet S. Kapoor ², Kanchan Jain ³

¹*Department of Statistics, Wachemo University, Ethiopia*

²*Department of Mathematics and Statistics, Central University of Punjab, India*

³*Department of Statistics, Panjab University, India*

Abstract The Kumaraswamy alpha power Lomax model, a five-parameter sub-model of the Kumaraswamy alpha power transformed family, is explored in detail. It is of particular interest because there are a variety of possible symmetrical and asymmetrical forms for the density function of this distribution. The proposed distribution is loaded with several features. Maximum likelihood, least squares, weighted least squares, and Cramer-von Mises are the four techniques used to estimate the parameters of the new model. A simulation study has been conducted to assess its effectiveness. Actuarial measures like value at risk and tail value at risk are also derived. Compared to other recently introduced heavy-tailed distributions, the tail of the proposed distribution is heavier. Moreover, the model's usefulness is investigated using four real data sets from the fields of insurance, finance, and reliability. Compared to other well-known Lomax-based and competing distributions, the results demonstrate that the proposed distribution can fit the data better.

Keywords Kumaraswamy distribution; Alpha power transformation; Lomax distribution; Heavy-tailed distribution; Actuarial measures

AMS 2010 subject classifications 62E10, 62F30

DOI: 10.19139/soic-2310-5070-2138

1. Introduction

The modeling of heavy-tailed data in applied fields has been investigated using heavy-tailed statistical distributions. Since data in the field of actuarial science, such as insurance losses, are frequently skewed to the right, unimodal, hump-shaped, and possess a thick right tail, researchers are primarily interested in distributions with only positive support. For details, one can refer to [7, 8, 9, 10, 11]. Classical distributions like the exponential, Rayleigh, Weibull, and Gamma cannot reveal extensive flexibility. These distributions are relatively limited in modeling heavy-tailed data for many reasons. Actuaries are constantly searching for new statistical distributions to fill in the gaps left by the traditional distributions because of the significance of heavy-tailed distributions in the field of actuarial sciences. According to Beirlant et al. [37], a distribution G is said to be heavy-tailed if

$$\lim_{x \rightarrow \infty} \frac{1 - G(x)}{e^{-\lambda x}} = \infty \text{ for all } \lambda > 0.$$

In risk management, heavy right-tailed distributions are useful for value at risk, tail value at risk, tail variance, and tail variance premium. In this context, Zhao et al. [38] introduced the heavy-tailed beta-power transformed Weibull distribution and compared it with other known distributions. The proposed model has been used to find

*Correspondence to: Wondimu Fikre (Email: wondiy2011@gmail.com). Department of Statistics, Wachemo University, 667 Hossana, Central Ethiopia, Ethiopia.

actuarial measures, and a simulation study has been carried out to establish the usefulness of the suggested model. The extended log-logistic distribution has been introduced to model heavy-tailed insurance loss data, and actuarial measures computed for the chosen models [39].

Recently, Ahmad et al. [40] contributed work on a particular sub-model of the proposed family, called the Weibull claim (W-Claim) model, and investigated its properties, characterizations, and applications to insurance claim data. Some risk measures are calculated for the fundamental Weibull and W-Claim distributions. According to the simulation study, the values of risk measures for the W-Claim distribution are larger than those for the conventional Weibull distribution. Arif et al. [41] developed extended heavy-tailed Weibull distribution, applying it to actuarial measures. They demonstrated the model's practical utility using heavy-tailed insurance loss data. The findings indicate that the proposed model outperforms six other competing models with respect to flexibility and efficiency.

Some related works recently introduced on this topic have different limitations. For example, Riad et al. [42] proposed a new heavy-tailed distribution called Kavya-Manoharan Power Lomax (KMPLo) with actuarial measures. They illustrated the suggested model using only one data set from the reliability field. Still, actuarial measures must be used to show how the model works in insurance, finance, and economics. Therefore, the potential flexibility and applicability of the proposed distribution in actuarial science and other domains is a significant gap in this work. The other heavy-tailed model recently introduced is the extended heavy-tailed Weibull (NEHTW) distribution [46]. However, the tail of the proposed distribution is compared with only the Weibull model, which is insufficient to suggest that the NEHTW model is a good candidate for heavy-tailed data sets. Other recently proposed heavy-tailed distributions in the literature are given in [43, 44, 45, 47, 48]. Given the above description, we are motivated to look for heavy-tailed distributions that are more flexible and improve the accuracy of data fitting in the fields of insurance, finance, reliabilities, and others. Kumaraswamy proposed a two-parameter distribution called Kumaraswamy distribution Kumaraswamy [1], denoted by $\text{Kum}(\psi, c)$. Its Cumulative Distribution Function (CDF) is given by

$$G(x) = 1 - (1 - x^\psi)^c, \quad 0 < x < 1, \psi, c > 0, \quad (1)$$

where $\psi, c > 0$ are shape parameters. However, Cordeiro and de Castro [12] extended the Kum distribution to a more generalized form and introduced the Kumaraswamy generalized (Kum-G) family of distributions with CDF and Probability Density Function (PDF) expressed as

$$G(x) = 1 - [1 - (F(x))^\psi]^c \quad (2)$$

and

$$g(x) = c\psi f(x)F(x)^{\psi-1}[1 - (F(x))^\psi]^{c-1}, \quad (3)$$

respectively, where $F(x)$ is the CDF of a chosen baseline distribution, with corresponding PDF $f(x)$.

The alpha power transformation (APT) family has been introduced by Mahdavi and Kundu [13]. If $L(x)$ is the CDF and $l(x)$ is the PDF of a continuous random variable X , then the CDF and PDF of this family are given by

$$F(x) = \begin{cases} \frac{a^{L(x)} - 1}{a - 1}, & x \in \mathbb{R}, a > 0, a \neq 1 \\ L(x), & a = 1, \end{cases} \quad (4)$$

$$f(x) = \begin{cases} \frac{(\log(a))}{a-1} l(x) a^{L(x)}, & a \neq 1 \\ l(x), & a = 1. \end{cases} \quad (5)$$

This technique provides more flexibility and enables a wider range of shapes by raising the base distribution to the power of a parameter. It applies in many disciplines where extreme values are widespread, such as reliability analysis, environmental sciences, and economics. Many novel distributions have been published in the literature using the alpha power transformation technique. Alpha power Lomax distribution was proposed by Bulut et al. [20], who investigated some distributional properties, but heavy-tailedness and flexibility of hazard rate function (hrf) were not addressed. A three-parameter alpha power transformed inverse Lomax distribution was introduced

by Zein et al. [21], which is more flexible than inverse Lomax distribution. Other recent distributions derived in the literature using alpha power transformation with different base distributions are alpha power Kum distribution [6], alpha power exponentiated Teissier distribution [4], alpha power exponentiated new Weibull-Pareto distribution [22], alpha power Kum-Burr III distribution [5] and alpha power inverse Weibull distribution [23]. The researchers are still focusing on deriving more generalized and flexible distributions that are superior to modified distributions using a combination of two or more techniques. Some flexible distributions generated from the combination of Kum-G and APT techniques in the literature are Kum alpha power inverted exponential distribution [2], alpha power Kum distribution [24] and alpha power inverted Kum distribution [25].

Lomax distribution was introduced by Lomax [14], and the CDF and PDF have the forms

$$L(x) = 1 - (1 + \varsigma x)^{-\vartheta}, x > 0, \varsigma, \vartheta > 0 \quad (6)$$

and

$$l(x) = \varsigma \vartheta (1 + \varsigma x)^{-(\vartheta+1)}, \quad (7)$$

respectively, where $\vartheta > 0$ and $\varsigma > 0$ are respectively shape and scale parameters. Lomax distribution is significant since it helps to deal with data with heavy tails. It is commonly used to model income distributions, insurance claim sizes, and product lifetimes where large values are relatively more frequent. Numerous distributions have been made available, utilizing the widely recognized Lomax distribution as a baseline. To cite a few, Kum-G power Lomax distribution [17], type II Topp-Leone power Lomax distribution [26], Kum-G inverse Lomax distribution [27], Marshall-Olkin alpha power Lomax distribution [3], power Lomax distribution [28], inverse power Lomax distribution [29] and Weibull-Lomax distribution [30].

This article aims to develop more generalized heavy-tailed distributions and evaluate the flexibility in modeling actuarial data and other fields. A novel five-parameter heavy-tailed distribution is proposed by combining the Kum-G and APT family of distributions. The proposed distribution is also known as the KAP-Lomax (Kumaraswamy alpha power Lomax distribution). The reasons behind choosing the combination of Kum-G and APT families to extend the Lomax distribution are:

- **Increased flexibility and control:** Combining both families makes it possible to describe complex data patterns in a more flexible manner. The Kum-G distribution provides a flexible base distribution with tractable features due to two shape parameters, allowing it to model a wide range of distribution shapes. At the same time, the APT alters the tail behavior and shape due to its transformation parameter.
- **Broad applicability:** When different kinds of tail behavior, skewness, and kurtosis are needed, the combination can provide distributions that are relevant in a variety of fields, including finance and environmental modeling.
- **Closed-form solutions:** Kum-G with APT family frequently yields distributions with closed-form PDFs and CDFs, which facilitate practical usage, particularly in parameter estimation, simulation, and hypothesis testing.
- **Modeling extreme events:** By merging these families, distributions that can effectively assess risk can be created in domains such as risk management. These distributions can be used to simulate both small and large losses.
- **Heavy-tailed nature and applicability of the Lomax distribution:** Lomax distribution is a continuous probability distribution with a heavy tail, which makes it convenient for modeling data in fields like finance, insurance, and reliability analysis, where extreme events are of particular concern.

The article is organized as follows. Section 2 introduces the Kumaraswamy alpha power transformed family of distributions and the sub-model, Kumaraswamy alpha power Lomax distribution. Some statistical properties of the Kumaraswamy alpha power Lomax distribution are explored in Section 3. In Section 4, estimation and simulation study are discussed. Section 5 provides the mathematical expressions of actuarial measures for the proposed model. Section 6 elaborates on the practical illustration using real data sets. Section 7 includes some concluding remarks.

2. Development of the Proposed Family

This section presents the Kumaraswamy alpha power transformed (KAPT) family of distributions. Using $L(x)$ as the CDF of any baseline distribution, the CDF of the KAPT family can be defined as

$$G(x) = \begin{cases} 1 - [1 - (\frac{a^{L(x)} - 1}{a - 1})^\psi]^c, & a \neq 1, c, a, \psi > 0, x > 0 \\ 1 - [1 - (L(x))^\psi]^c, & a = 1. \end{cases} \tag{8}$$

From (8), the KAPT family reduces to

- the Kum-G family for $a = 1$,
- the APT family for $c = \psi = 1$,
- the exponentiated family for $a = c = 1$.

The PDF of the KAPT family corresponding to (8) is

$$g(x) = \begin{cases} \frac{(\log(a))}{a-1} c\psi l(x) a^{L(x)} (\frac{a^{L(x)} - 1}{a - 1})^{\psi-1} [1 - (\frac{a^{L(x)} - 1}{a - 1})^\psi]^{c-1}, & a \neq 1 \\ c\psi l(x) L(x)^{\psi-1} [1 - L(x)^\psi]^{c-1}, & a = 1. \end{cases} \tag{9}$$

It is possible to derive new flexible distributions using the forms of CDF, $L(x)$, and PDF, $l(x)$ in equation (8).

2.1. The Kumaraswamy Alpha Power Lomax Distribution

This section introduces a five-parameter KAP-Lomax distribution that significantly contributes to the insurance, finance, and reliability fields by providing a robust and flexible tool for modeling light and heavy-tailed data. The KAP-Lomax distribution is desirable for contemporary risk management, pricing, and financial analytics because of its adaptability, closed-form solutions, and flexibility.

Using equations (2), (4) and (6), a random variable X is said to have KAP-Lomax distribution if its CDF is

$$G(x, \Pi) = \begin{cases} 1 - \left[1 - \left(\frac{a^{1-(1+\zeta x)^{-\vartheta}} - 1}{a - 1} \right)^\psi \right]^c, & a \neq 1, a, c, \zeta, \psi, \vartheta > 0, x > 0 \\ 1 - [1 - (1 - (1 + \zeta x)^{-\vartheta})^\psi]^c, & a = 1, \end{cases} \tag{10}$$

where $\Pi = (a, c, \zeta, \psi, \vartheta)'$, $\vartheta, \psi, c > 0$ are shape parameters.

Comprehending and interpreting the parameters of the KAP-Lomax distribution in real-world applications needs breaking down its components and considering how they might be applied practically. The shape parameters ψ and c determine the shape of the distribution, particularly the skewness and tail behavior. In reliability engineering, they are used to model the life span of a product, where ψ and c control how quickly the probability of failure increases or decreases over time. The parameter a of APT influences the distribution's shape by adjusting the heaviness of the tail and the peak. Higher values of a can make the distribution more skewed or heavy-tailed. In finance, a can model the behavior of extreme events, like market crashes, by affecting how likely extreme returns are. The scale parameter ζ influences the spread of the distribution. A larger ζ means that values are more spread out. Risk assessment might represent the scale of losses in case of a catastrophic event, and a larger value would imply that extreme losses are more likely. The shape parameter ϑ mainly affects the tail behavior of the distribution. It is essential to model how rapidly the probability decreases as we move away from the mode. In insurance, ϑ could be used to model the distribution of claim sizes, whereas a higher value could indicate a slower decay in the probability of extremely large claims.

We write $G(x)$ in the place of $G(x, \Pi)$ and $g(x)$ in the place of $g(x, \Pi)$ for simplicity. The PDF, the survival function, and the hrf of KAP-Lomax distribution corresponding to (10) are, respectively, written as

$$g(x) = \begin{cases} \frac{(\log(a))}{a-1} c\psi\zeta\vartheta(1 + \zeta x)^{-(\vartheta+1)} a^{1-(1+\zeta x)^{-\vartheta}} (\frac{a^{1-(1+\zeta x)^{-\vartheta}} - 1}{a - 1})^{\psi-1} [1 - (\frac{a^{1-(1+\zeta x)^{-\vartheta}} - 1}{a - 1})^\psi]^{c-1} \\ c\psi\zeta\vartheta(1 + \zeta x)^{-(\vartheta+1)} (1 - (1 + \zeta x)^{-\vartheta})^{\psi-1} [1 - (1 - (1 + \zeta x)^{-\vartheta})^\psi]^{c-1}, & a \neq 1 \end{cases} \tag{11}$$

$$S(x) = 1 - G(x) = \left[1 - \left(\frac{a^{1-(1+\zeta x)^{-\vartheta}} - 1}{a - 1} \right)^\psi \right]^c, \quad a \neq 1, \tag{12}$$

and

$$h(x) = \frac{\frac{\log(a)}{(a-1)} c \psi \zeta \vartheta (1 + \zeta x)^{-(\vartheta+1)} a^{1-(1+\zeta x)^{-\vartheta}} \left(\frac{a^{1-(1+\zeta x)^{-\vartheta}} - 1}{a - 1} \right)^{\psi-1}}{1 - \left(\frac{a^{1-(1+\zeta x)^{-\vartheta}} - 1}{a - 1} \right)^\psi}, \quad a \neq 1. \tag{13}$$

3. Basic Properties of KAP-Lomax Distribution

The plots of PDF, CDF, survival, and hrf of KAP-Lomax for various combinations of parameters are shown in Figures 1, 2, 3 and 4, respectively. The plots of PDF in Figures 1 and 2 suggest that the proposed distribution is positively skewed and unimodal for $\psi > 1$. In Figures 1(a), 1(b) and 2(b), the suggested model tends toward a heavy-tailed distribution as the values of the shape parameters c and ϑ decrease. From Figure 2(a), it is clear that as the value of the shape parameter ψ increases, the right tail of the KAP-Lomax distribution tends to assign higher probabilities to larger values, indicating that the proposed model tends to be heavy-tailed. Figure 4 depicts that the proposed distribution has reversed symmetric densities, decreasing/increasing, bathtub, upside-down bathtub shaped, and constant and reversed-J hazard rates.

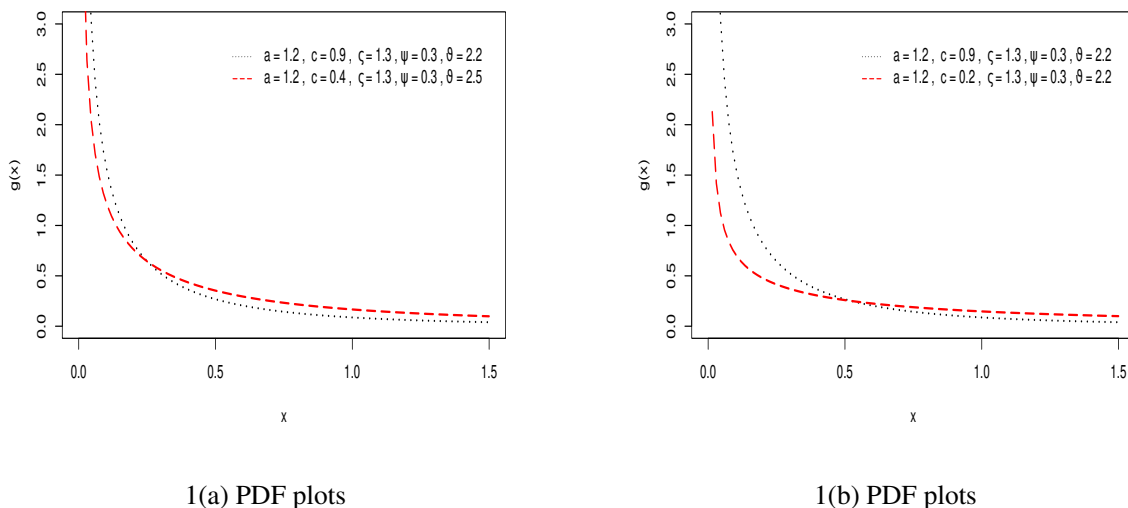


Figure 1. The PDF plots of the KAP-Lomax.

3.1. Quantile Function

The ρ^{th} quantile of KAP-Lomax distribution is derived as

$$x_\rho = \frac{1}{\zeta} \left\{ \left(\frac{\log(a)}{\log(a) - \log(1 + (a - 1)[1 - (1 - \rho)^{\frac{1}{c}}]^{\frac{1}{\psi}})} \right)^{\frac{1}{\vartheta}} \right\}, \tag{14}$$

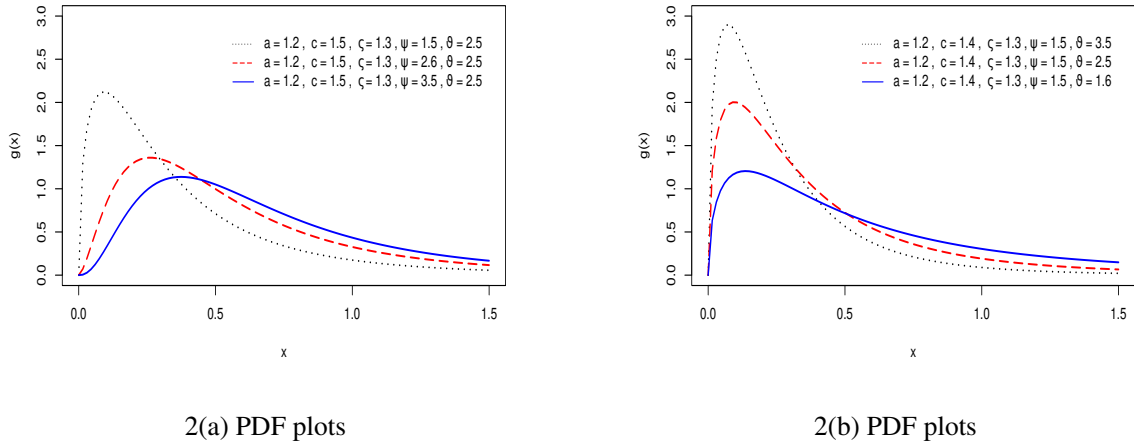


Figure 2. The PDF plots of the KAP-Lomax.

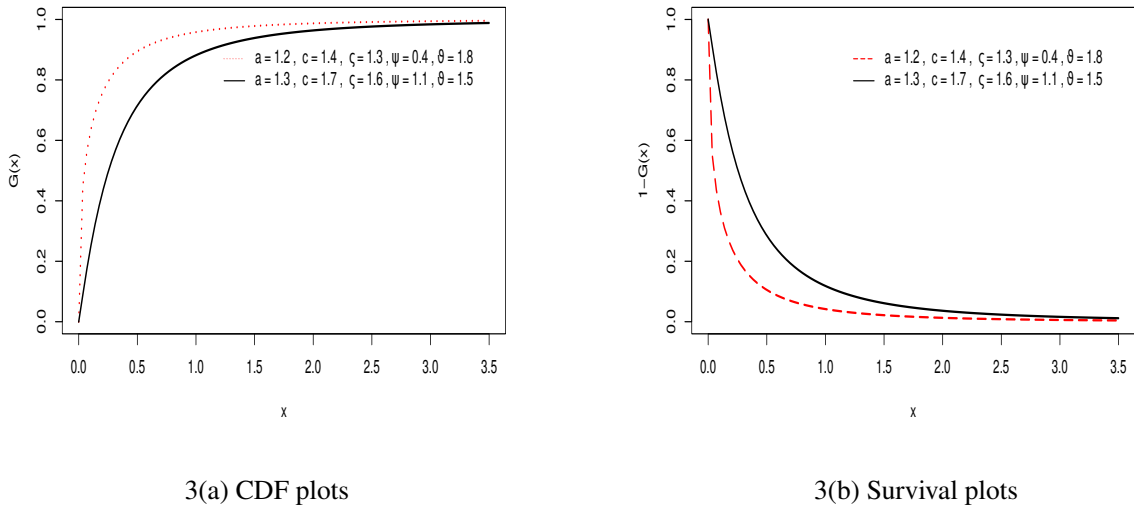


Figure 3. The CDF and survival function plots of the KAP-Lomax.

where $0 < \rho < 1, a \neq 1, a, c, \zeta, \psi, \vartheta > 0$. Replacing ρ by $(0.25, 0.5, 0.75)$ in (14), the first quartile (Q_1), the second quartile (Q_2), and third quartile (Q_3) of KAP-Lomax distribution can be, respectively written as follows:

$$\begin{aligned}
 Q_1 &= \frac{1}{\zeta} \left\{ \left(\frac{\log(a)}{\log(a) - \log(1 + (a-1)[1 - (1-1/4)^{\frac{1}{\zeta}}]^{\frac{1}{\psi}})} \right)^{\frac{1}{\vartheta}} \right\} \\
 Q_2 &= \frac{1}{\zeta} \left\{ \left(\frac{\log(a)}{\log(a) - \log(1 + (a-1)[1 - (1-1/2)^{\frac{1}{\zeta}}]^{\frac{1}{\psi}})} \right)^{\frac{1}{\vartheta}} \right\} \\
 Q_3 &= \frac{1}{\zeta} \left\{ \left(\frac{\log(a)}{\log(a) - \log(1 + (a-1)[1 - (1-3/4)^{\frac{1}{\zeta}}]^{\frac{1}{\psi}})} \right)^{\frac{1}{\vartheta}} \right\}.
 \end{aligned}
 \tag{15}$$

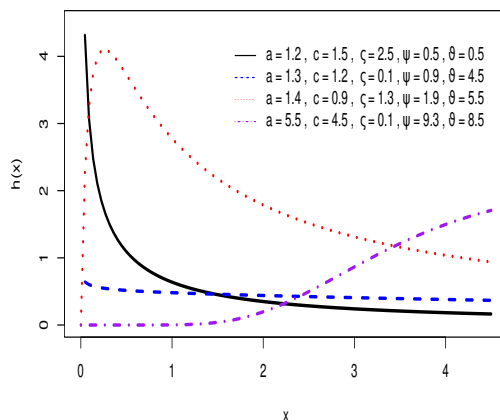


Figure 4. The hrf plots of the KAP-Lomax.

3.2. Skewness and Kurtosis

The shapes of KAP-Lomax distribution can be obtained using Galton’s skewness and Moor’s kurtosis [15]. These are obtained using (14 and 15), as follows:

$$Skewness = \frac{Q_3 - 2Q_2 + Q_1}{Q_3 - Q_1}, \tag{16}$$

and

$$Kurtosis = \frac{x_{.875} - x_{.625} + x_{.375} - x_{.125}}{Q_3 - Q_1}. \tag{17}$$

3.3. Moment Generating Function (mgf)

If $X \sim \text{KAP-Lomax}(a, c, \zeta, \psi, \vartheta)$, the mgf is expressed as

$$M_X(t) = \sum_{b, \ell, k=0}^{\infty} \sum_{r=1}^{\infty} \frac{t^r}{r!} v_{b, \ell}(\Pi, 1) \frac{(-1)^{1+r} e^{(\ell+1)\log(a)} a^{\ell+1} \zeta^{-r-1} \zeta(1+r) \zeta(\vartheta - k\vartheta)}{\zeta(1+r+\vartheta - k\vartheta)}. \tag{18}$$

Moments

For any positive integer r , the r^{th} order moment about the origin is provided as follows:

$$\mu'_r = E[X^r] = \int_0^{\infty} x^r g(x) dx. \tag{19}$$

This integral is not tractable given the mathematical complexity of the density function in (19). The expansion for the PDF of the KAP-Lomax may be obtained using an analytical approach and can be plugged into (19). The following result displays a series expansion of a power transformation of the KAP-Lomax distribution’s PDF.

Proposition 3.1

For any $\hbar > 0$,

$$(g(x, \Pi))^{\hbar} = \sum_{b=0}^{\infty} \sum_{\ell=0}^{\infty} v_{b,\ell}(\Pi, \hbar) d_{\ell}(x, a, \varsigma, \vartheta, \hbar), x > 0,$$

where

$$v_{b,\ell}(\Pi, \hbar) = \left(\frac{\log(a)}{a-1} c\psi\varsigma\vartheta\right)^{\hbar} \left(\frac{1}{1-a}\right)^{\psi b + \hbar - 1} \binom{\hbar(c-1)}{b} \binom{\psi b + \hbar(\psi-1)}{\ell} (-1)^{b+\ell},$$

and

$$d_{\ell}(x, a, \varsigma, \vartheta, \hbar) = (1 + \varsigma x)^{-\hbar(\vartheta+1)} a^{(\ell+\hbar)[1-(1+\varsigma x)^{-\vartheta}]}$$

are generalized binomial coefficients.

Proof

We have

$$(g(x, \Pi))^{\hbar} = \left(\frac{\log(a)}{a-1} c\psi\varsigma\vartheta\right)^{\hbar} (1 + \varsigma x)^{-\hbar(\vartheta+1)} a^{\hbar[1-(1+\varsigma x)^{-\vartheta}]} \left(\frac{a^{1-(1+\varsigma x)^{-\vartheta}} - 1}{a-1}\right)^{\hbar(\psi-1)} \left[1 - \left(\frac{a^{1-(1+\varsigma x)^{-\vartheta}} - 1}{a-1}\right)^{\psi}\right]^{\hbar(c-1)}.$$

Now, we use the result which gives $(1 - \aleph)^n = \sum_{b=0}^{\infty} \binom{n}{b} (-1)^b \aleph^b$ for any real number n and \aleph such that $|\aleph| < 1$. Therefore, by applying this result, we obtain

$$\begin{aligned} (g(x, \Pi))^{\hbar} &= \left(\frac{\log(a)}{a-1} c\psi\varsigma\vartheta\right)^{\hbar} (1 + \varsigma x)^{-\hbar(\vartheta+1)} a^{\hbar[1-(1+\varsigma x)^{-\vartheta}]} \sum_{b=0}^{\infty} \binom{\hbar(c-1)}{b} (-1)^b \\ &\quad \left(\frac{a^{1-(1+\varsigma x)^{-\vartheta}} - 1}{a-1}\right)^{\psi b + \hbar(\psi-1)}. \\ &= \left(\frac{\log(a)}{a-1} c\psi\varsigma\vartheta\right)^{\hbar} (1 + \varsigma x)^{-\hbar(\vartheta+1)} \sum_{b=0}^{\infty} \sum_{\ell=0}^{\infty} \binom{\hbar(c-1)}{b} \binom{\psi b + \hbar(\psi-1)}{\ell} (-1)^{b+\ell} \\ &\quad a^{(\ell+\hbar)[1-(1+\varsigma x)^{-\vartheta}]} \left(\frac{1}{a-1}\right)^{\psi b + \hbar - 1}. \\ &= \sum_{b=0}^{\infty} \sum_{\ell=0}^{\infty} v_{b,\ell}(\Pi, \hbar) d_{\ell}(x, a, \varsigma, \vartheta, \hbar). \end{aligned}$$

□

For $\hbar = 1$, Proposition (3.1) gives

$$g(x, \Pi) = \sum_{b=0}^{\infty} \sum_{\ell=0}^{\infty} v_{b,\ell}(\Pi, 1) d_{\ell}(x, a, \varsigma, \vartheta, 1).$$

Hence X has r^{th} order moment about the origin written as

$$\mu'_r = \int_0^{\infty} x^r \left[\sum_{b=0}^{\infty} \sum_{\ell=0}^{\infty} v_{b,\ell}(\Pi, 1) d_{\ell}(x, a, \varsigma, \vartheta, 1) \right] dx = \sum_{b=0}^{\infty} \sum_{\ell=0}^{\infty} v_{b,\ell}(\Pi, 1) \int_0^{\infty} x^r d_{\ell}(x, a, \varsigma, \vartheta, 1) dx.$$

The integral term can be expressed as

$$\int_0^{\infty} x^r d_{\ell}(x, a, \varsigma, \vartheta, 1) dx = \int_0^{\infty} x^r (1 + \varsigma x)^{-(\vartheta+1)} a^{(\ell+1)[1-(1+\varsigma x)^{-\vartheta}]} dx$$

Set $y = (1 + \varsigma x)^{-\vartheta}$, so $x = \frac{1}{\varsigma} (y^{-\frac{1}{\vartheta}} - 1)$ and $\partial x = \frac{-1}{\varsigma \vartheta y^{\frac{1}{\vartheta}+1}} \partial y$, where $0 < y < 1$. Then

$$\int_0^{\infty} x^r (1 + \varsigma x)^{-(\vartheta+1)} a^{(\ell+1)[1-(1+\varsigma x)^{-\vartheta}]} dx = \frac{-a^{\ell+1}}{\vartheta \varsigma^{r+1}} \int_0^1 \frac{(y^{\frac{1}{\vartheta}} - 1)^r}{a^{y(\ell+1)}} \partial y.$$

Since $a^z = \sum_{k=0}^{\infty} \frac{(\log(a))^k}{k!} Z^k$, hence the above expression can be written as

$$\begin{aligned} \frac{-a^{\ell+1}}{\vartheta \varsigma^{r+1}} \int_0^1 \frac{(y^{\frac{1}{\vartheta}} - 1)^r}{a^{y(\ell+1)}} \partial y &= \frac{-a^{\ell+1}}{\vartheta \varsigma^{r+1}} \sum_{k=0}^{\infty} \frac{(\log(a))^k}{k!} (\ell+1)^k \int_0^1 \frac{(y^{\frac{1}{\vartheta}} - 1)^r}{y^k} \partial y \\ &= \frac{(-1)^{1+r} e^{(\ell+1)\log(a)} a^{\ell+1} \varsigma^{-r-1} \varsigma(1+r) \varsigma(\vartheta - k\vartheta)}{\varsigma(1+r+\vartheta - k\vartheta)}. \end{aligned}$$

Finally, we get

$$\mu'_r = \sum_{b=0}^{\infty} \sum_{\ell=0}^{\infty} \sum_{k=0}^{\infty} v_{b,\ell}(\Pi, 1) \frac{(-1)^{1+r} e^{(\ell+1)\log(a)} a^{\ell+1} \varsigma^{-r-1} \varsigma(1+r) \varsigma(\vartheta - k\vartheta)}{\varsigma(1+r+\vartheta - k\vartheta)}.$$

Proposition 3.2

For any $\lambda > 0$,

$$\lim_{x \rightarrow \infty} \frac{1 - G(x, \Pi)}{e^{-\lambda x}} = \lim_{x \rightarrow \infty} \frac{\left(1 - \left(\frac{a^{1-(1+\varsigma x)^{-\vartheta}} - 1}{a-1}\right)^{\psi}\right)^c}{e^{-\lambda x}} = \infty.$$

Proof

To show that

$$\lim_{x \rightarrow \infty} e^{\lambda x} \left(1 - \left(\frac{a^{1-(\varsigma x+1)^{-\vartheta}} - 1}{a-1}\right)^{\psi}\right)^c = \infty,$$

for $a > 0$, $\varsigma > 0$, $\vartheta > 0$, $\psi > 0$, and $c > 0$, let's analyze the behavior of the expression as $x \rightarrow \infty$.

Step 1: Consider the expression inside the parentheses:

$$\frac{a^{1-(\varsigma x+1)^{-\vartheta}} - 1}{a-1}.$$

As $x \rightarrow \infty$: $(\varsigma x + 1)^{-\vartheta} \rightarrow 0$, because $\varsigma x + 1 \rightarrow \infty$ and raising a large number to a negative power, it tends to zero. Thus, $1 - (\varsigma x + 1)^{-\vartheta} \rightarrow 1$. So the expression becomes:

$$a^{1-(\varsigma x+1)^{-\vartheta}} \rightarrow a^1 = a.$$

Hence:

$$\frac{a^{1-(\varsigma x+1)^{-\vartheta}} - 1}{a-1} \rightarrow \frac{a-1}{a-1} = 1.$$

Step 2: Raise the above expression to the power ψ :

$$\left(\frac{a^{1-(\varsigma x+1)^{-\vartheta}} - 1}{a-1}\right)^{\psi} \rightarrow 1^{\psi} = 1.$$

Step 3: Now subtract the expression from 1:

$$1 - \left(\frac{a^{1-(\varsigma x+1)^{-\vartheta}} - 1}{a - 1} \right)^\psi \rightarrow 1 - 1 = 0.$$

Step 4: Raise the result to the power c :

$$\left(1 - \left(\frac{a^{1-(\varsigma x+1)^{-\vartheta}} - 1}{a - 1} \right)^\psi \right)^c \rightarrow 0^c = 0.$$

Step 5: Now multiply this by $e^{\lambda x}$:

$$e^{\lambda x} \left(1 - \left(\frac{a^{1-(\varsigma x+1)^{-\vartheta}} - 1}{a - 1} \right)^\psi \right)^c.$$

Given that $e^{\lambda x}$ grows exponentially as $x \rightarrow \infty$, and the other factor tends to 0, we need to determine the overall limit. Thus, although the term $\left(1 - \left(\frac{a^{1-(\varsigma x+1)^{-\vartheta}} - 1}{a - 1} \right)^\psi \right)^c$ tends to 0, the exponential term $e^{\lambda x}$ grows very rapidly. Therefore, the exponential term dominates the product, causing the entire expression to approach infinity. Thus,

$$\lim_{x \rightarrow \infty} e^{\lambda x} \left(1 - \left(\frac{a^{1-(\varsigma x+1)^{-\vartheta}} - 1}{a - 1} \right)^\psi \right)^c = \infty.$$

□

4. Estimation and Simulation Study

The estimation techniques maximum likelihood, least squares, weighted least squares, and Cramer-von Mises have been implemented for the parameter estimation of the KAP-Lomax distribution, and a simulation study carried out.

4.1. Maximum Likelihood Estimation (MLE)

Let x_1, x_2, \dots, x_n be a random sample from KAP-Lomax distribution. Then the log-likelihood function for the parameter vector $\Pi = (a, c, \varsigma, \psi, \vartheta)$, using the PDF in (11) is,

$$l(\Pi) = n \log \left(\frac{\log(a)}{a - 1} \right) + n \log(c\psi\varsigma\vartheta) - (\vartheta + 1) \sum_{b=1}^n \log(1 + \varsigma x_b) + \log(a) \sum_{b=1}^n [1 - (1 + \varsigma x_b)^{-\vartheta}] + (\psi - 1) \sum_{b=1}^n \log \left(\frac{a^{1-(1+\varsigma x_b)^{-\vartheta}} - 1}{a - 1} \right) + (c - 1) \sum_{b=1}^n \log \left[1 - \left(\frac{a^{1-(1+\varsigma x_b)^{-\vartheta}} - 1}{a - 1} \right)^\psi \right]. \tag{20}$$

The MLEs are computed by equating the first partial derivatives, $\frac{\partial l(\Pi)}{\partial a}$, $\frac{\partial l(\Pi)}{\partial c}$, $\frac{\partial l(\Pi)}{\partial \varsigma}$, $\frac{\partial l(\Pi)}{\partial \psi}$ and $\frac{\partial l(\Pi)}{\partial \vartheta}$ of the log-likelihood function with respect to a, c, ς, ψ and ϑ to zeros and solving for the parameters a, c, ς, ψ and ϑ .

4.2. Least square estimation (LSE)

Let the order statistics of a random sample from KAP-Lomax be $x_{1:m}, x_{2:m}, \dots, x_{m:m}$. Then, the LSE of the parameters of the KAP-Lomax distribution is obtained by minimizing the equation written as (21).

$$L = \sum_{b=1}^m \left[G(x_{b:m}) - \frac{b}{m + 1} \right]^2 = \sum_{b=1}^m \left[1 - \left(1 - \left(\frac{a^{1-(\varsigma x_b+1)^{-\vartheta}} - 1}{a - 1} \right)^\psi \right)^c - \frac{b}{m + 1} \right]^2. \tag{21}$$

It is also possible to derive the LSE of the KAP-Lomax parameters by resolving the following equations:

$$\sum_{b=1}^m \left[1 - \left(1 - \left(\frac{a^{1-(\zeta x_b+1)^{-\vartheta}} - 1}{a-1} \right)^{\psi} \right)^c - \frac{b}{m+1} \right] \delta_k(x_{b:m}) = 0, k = 1, 2, 3, 4, 5 \quad (22)$$

where

$$\delta_1(x_{b:m}) = \frac{\partial}{\partial a} G(x_{b:m}) = c\psi \left(\frac{(1 - (\zeta x + 1)^{-\vartheta}) a^{-(\zeta x+1)^{-\vartheta}} - a^{1-(\zeta x+1)^{-\vartheta}} - 1}{(a-1)^2} \right) \left(\frac{a^{1-(\zeta x+1)^{-\vartheta}} - 1}{a-1} \right)^{\psi-1} \left(1 - \left(\frac{a^{1-(\zeta x+1)^{-\vartheta}} - 1}{a-1} \right)^{\psi} \right)^{c-1}, \quad (23)$$

$$\delta_2(x_{b:m}) = \frac{\partial}{\partial \zeta} G(x_{b:m}) = c\vartheta x \psi \frac{\log(a)}{a-1} (\zeta x + 1)^{-\vartheta-1} a^{1-(\zeta x+1)^{-\vartheta}} \left(\frac{a^{1-(\zeta x+1)^{-\vartheta}} - 1}{a-1} \right)^{\psi-1} \left(1 - \left(\frac{a^{1-(\zeta x+1)^{-\vartheta}} - 1}{a-1} \right)^{\psi} \right)^{c-1}, \quad (24)$$

$$\delta_3(x_{b:m}) = \frac{\partial}{\partial \vartheta} G(x_{b:m}) = c\psi \frac{\log(a)}{a-1} (\zeta x + 1)^{-\vartheta} \log(\zeta x + 1) a^{1-(\zeta x+1)^{-\vartheta}} \left(\frac{a^{1-(\zeta x+1)^{-\vartheta}} - 1}{a-1} \right)^{\psi-1} \left(1 - \left(\frac{a^{1-(\zeta x+1)^{-\vartheta}} - 1}{a-1} \right)^{\psi} \right)^{c-1}, \quad (25)$$

$$\delta_4(x_{b:m}) = \frac{\partial}{\partial \psi} G(x_{b:m}) = c \left(\frac{a^{1-(\zeta x+1)^{-\vartheta}} - 1}{a-1} \right)^{\psi} \log \left(\frac{a^{1-(\zeta x+1)^{-\vartheta}} - 1}{a-1} \right) \left(1 - \left(\frac{a^{1-(\zeta x+1)^{-\vartheta}} - 1}{a-1} \right)^{\psi} \right)^{c-1}, \quad (26)$$

$$\delta_5(x_{b:m}) = \frac{\partial}{\partial c} G(x_{b:m}) = - \left(1 - \left(\frac{a^{1-(\zeta x+1)^{-\vartheta}} - 1}{a-1} \right)^{\psi} \right)^c \log \left(1 - \left(\frac{a^{1-(\zeta x+1)^{-\vartheta}} - 1}{a-1} \right)^{\psi} \right). \quad (27)$$

4.3. Weighted least square estimation (WLSE)

By minimizing W, the WLSE of the KAP-Lomax parameters can be obtained where

$$W = \sum_{b=1}^m \frac{(m+1)^2(m+2)}{b(m-b+1)} \left[G(x_{b:m}) - \frac{b}{m+1} \right]^2 = \sum_{b=1}^m \frac{(m+1)^2(m+2)}{b(m-b+1)} \left[1 - \left(1 - \left(\frac{a^{1-(\zeta x_b+1)^{-\vartheta}} - 1}{a-1} \right)^{\psi} \right)^c - \frac{b}{m+1} \right]^2. \quad (28)$$

4.4. Cramer-von Mises Estimation (CVME)

The CVME of KAP-Lomax parameters are obtained by minimizing the following equation:

$$CV = \frac{1}{12m} + \sum_{b=1}^m \left[G(x_{b:m}) - \frac{2b-1}{2m} \right]^2 = \frac{1}{12m} + \sum_{b=1}^m \left[1 - \left(1 - \left(\frac{a^{1-(\zeta x_b+1)^{-\vartheta}} - 1}{a-1} \right)^{\psi} \right)^c - \frac{2b-1}{2m} \right]^2. \quad (29)$$

Alternatively, through resolving the subsequent equations:

$$\sum_{b=1}^m \left[1 - \left(1 - \left(\frac{a^{1-(\zeta x_b + 1)^{-\vartheta}} - 1}{a - 1} \right)^\psi \right)^c - \frac{2b - 1}{2m} \right] \delta_k(x_{b:m}) = 0, \tag{30}$$

where $\delta_k(x_{b:m})$, for $k = 1, 2, 3, 4, 5$, are defined in equations (23-27).

4.5. Simulation Study

In this subsection, the performance of the estimates obtained by the four estimation methods is evaluated by performing a simulation study. The steps are as follows:

- (1) Samples X_1, X_2, \dots, X_n of sizes $n = 25, 50, 100, \dots, 500$ from the KAP-Lomax are generated.
- (2) the MLEs, LSEs, WLSEs, and CVMEs are computed.
- (3) Ten thousand repetitions are performed to compute the estimates' mean square error (MSE) and the absolute bias (AB).
- (4) Two combinations of values are considered for the parameters of the KAP-Lomax distribution.

The simulation results are shown numerically in Tables 1, 2, and 3, and the results of MLEs, LSEs, WLSEs, and CVMEs with their corresponding MSEs are graphically displayed in Figures 5-12. From the numerical and graphical results, it can be noted that as sample size rises

- (i) the values of the estimates get closer and closer to the parameters $(a, c, \zeta, \psi, \vartheta)$ and
- (ii) the values of the MSE and AB of the estimates tend to zero for all the four estimation methods.

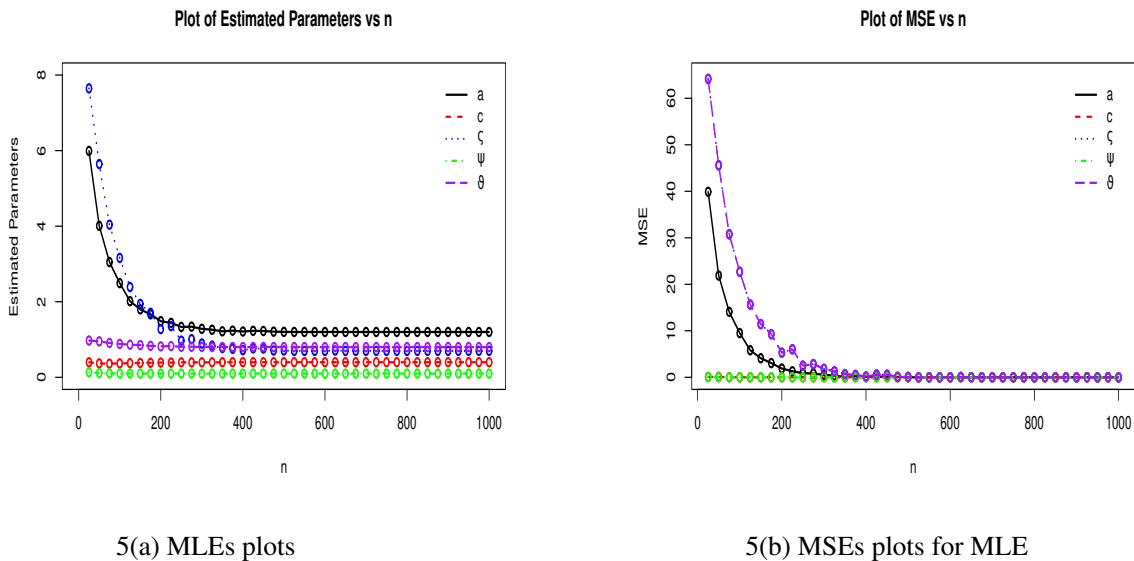


Figure 5. Plots of MLEs and MSEs of the KAP-Lomax for $a = 1.2, c = 0.4, \zeta = 0.7, \psi = 0.1, \vartheta = 0.8$.

5. Actuarial Measures

Analyzing an instrument portfolio's vulnerability to market risk in actuarial sciences is one of the most important tasks. Risk may arise from changes in underlying variables such as prices of equity and interest rates/exchange rates. Using the proposed distribution, this section computed the Value at Risk (VaR) and Tail Value at Risk (TVaR).

Table 1. MLE, LSE, WLSE, CVME of KAP-Lomax for two combinations of parameters (Par.)

		$a = 1.2, c = .4, \varsigma = .7, \psi = .1, \vartheta = .8$				$a = 1.3, c = .2, \varsigma = .9, \psi = .1, \vartheta = .3$			
n	Par.	MLE	LSE	WLSE	CVME	MLE	LSE	WLSE	CVME
25	\hat{a}	5.591	6.259	7.615	1.426	3.186	7.747	1.388	1.647
	\hat{c}	0.414	0.205	0.102	0.132	0.328	0.049	4.043	0.035
	$\hat{\varsigma}$	7.361	0.313	0.189	0.855	7.662	0.224	1.339	0.475
	$\hat{\psi}$	0.129	5.822	7.316	5.217	0.274	7.536	0.022	8.049
	$\hat{\vartheta}$	0.966	0.403	0.209	0.774	0.398	0.074	0.498	0.091
50	\hat{a}	4.105	4.293	6.154	1.502	2.526	6.345	1.615	1.747
	\hat{c}	0.355	0.271	0.175	0.200	0.248	0.075	3.327	0.060
	$\hat{\varsigma}$	5.658	0.460	0.309	0.951	6.663	0.378	1.178	0.468
	$\hat{\psi}$	0.108	3.583	5.673	3.10	0.159	5.840	0.039	5.308
	$\hat{\vartheta}$	0.961	0.541	0.353	1.142	0.363	0.113	0.397	0.199
100	\hat{a}	2.701	1.507	3.848	1.591	1.948	3.294	1.557	1.904
	\hat{c}	0.367	0.297	0.280	0.280	0.214	0.104	1.997	0.101
	$\hat{\varsigma}$	3.405	0.664	0.490	0.680	4.981	0.692	1.045	0.595
	$\hat{\psi}$	0.103	0.437	3.079	1.678	0.120	2.365	0.065	3.446
	$\hat{\vartheta}$	0.877	0.749	0.559	0.813	0.330	0.201	0.342	0.207
200	\hat{a}	1.529	1.228	1.833	1.399	1.354	1.589	1.501	1.767
	\hat{c}	0.391	0.369	0.371	0.367	0.199	0.153	0.906	0.154
	$\hat{\varsigma}$	1.332	0.693	0.649	0.673	1.145	0.869	0.961	0.782
	$\hat{\psi}$	0.100	0.128	0.812	0.494	0.100	0.428	0.086	1.394
	$\hat{\vartheta}$	0.818	0.789	0.742	0.765	0.300	0.293	0.310	0.240
500	\hat{a}	1.213	1.200	1.208	1.204	1.305	1.311	1.308	1.371
	\hat{c}	0.399	0.399	0.399	0.399	0.200	0.191	0.233	0.197
	$\hat{\varsigma}$	0.718	0.699	0.699	0.699	0.918	0.898	0.912	0.892
	$\hat{\psi}$	0.100	0.100	0.109	0.104	0.100	0.112	0.099	0.181
	$\hat{\vartheta}$	0.800	0.799	0.799	0.799	0.299	0.292	0.300	0.295

5.1. Value at Risk (VaR)

Practitioners widely use the measure VaR as a standard financial risk instrument in the context of actuarial sciences. Alternatively, VaR is referred to as the quantile risk measure, and it is expressed with a confidence level, say ρ (usually 90%, 95%, or 99%). VaR of a random variable X is the ρ^{th} quantile of the CDF [16]. If $X \sim \text{KAP-Lomax}(x; \Pi)$ for $\Pi = (a, c, \varsigma, \psi, \vartheta)'$, then the VaR of X at the $100\rho\%$ level denoted by $VaR_\rho(X)$ is the value of π_ρ satisfying

$$Pr(X > \pi_\rho) = 1 - \rho, \quad 0 < \rho < 1.$$

Using the quantile function, the VaR can be derived as

$$VaR_\rho(X) = \frac{1}{\varsigma} \left\{ \left(\frac{\log(a)}{\log(a) - \log(1 + (a - 1)[1 - (1 - \rho)^{\frac{1}{c}}])^{\frac{1}{\psi}}} \right)^{\frac{1}{\vartheta}} \right\}, \tag{31}$$

where $0 < \rho < 1, a, c, \varsigma, \vartheta, \psi > 0$ and $a \neq 1$.

Table 2. MSE of KAP-Lomax for two combinations of parameters.

n	Par.	a = 1.2, c = .4, ζ = .7, ψ = .1, ϑ = .8				a = 1.3, c = .2, ζ = .9, ψ = .1, ϑ = .3				
		MLE	LSE	WLSE	CVME	MLE	LSE	WLSE	CVME	
25	MSE	\hat{a}	36.4921	0.3814	56.1600	0.1707	15.2810	52.2201	1.6151	0.1513
		\hat{c}	0.1303	0.0712	0.1186	0.1066	0.3127	0.0283	19.2595	0.0326
		$\hat{\zeta}$	61.4131	0.2321	0.3547	1.2049	59.2047	0.5709	1.4043	0.2256
		$\hat{\psi}$	0.0303	0.4864	71.0723	44.8242	0.4477	69.2420	0.0076	77.5708
		$\hat{\vartheta}$	0.4169	0.2869	0.4695	0.8053	0.0775	0.0638	0.0777	0.0731
50	MSE	\hat{a}	22.7268	0.2015	43.5974	0.2703	8.6613	38.6851	2.4447	0.3490
		\hat{c}	0.0307	0.0385	0.0894	0.0795	0.2176	0.0223	16.0506	0.0277
		$\hat{\zeta}$	45.7978	0.1231	0.2713	0.8425	51.2157	0.4132	1.3433	0.3904
		$\hat{\psi}$	0.0009	0.2554	55.1782	20.4117	0.0866	50.0867	0.0060	44.1435
		$\hat{\vartheta}$	0.2803	0.1528	0.3550	0.6936	0.0304	0.0501	0.289	0.0376
100	MSE	\hat{a}	11.1614	1.9646	23.3094	0.5596	3.4120	16.9694	1.9424	0.8511
		\hat{c}	0.0071	0.0401	0.0477	0.0473	0.0599	0.0187	9.5190	0.0195
		$\hat{\zeta}$	24.9619	0.0135	0.1465	0.1381	36.6469	0.1812	0.8051	0.2128
		$\hat{\psi}$	0.0003	2.4792	29.5009	8.8903	0.0022	21.9724	0.0033	25.8080
		$\hat{\vartheta}$	0.1152	0.0203	0.1914	0.0748	0.0099	0.0238	0.0091	0.0218
200	MSE	\hat{a}	2.3528	0.0175	5.5756	0.4907	0.1868	2.3788	1.5153	1.0191
		\hat{c}	0.0016	0.0120	0.0114	0.0127	0.0000	0.0092	3.7155	0.0085
		$\hat{\zeta}$	5.7930	0.0005	0.0351	0.0088	2.2346	0.0254	0.2806	0.0649
		$\hat{\psi}$	0.0000	0.0194	7.0567	1.9231	0.0000	3.0800	0.0013	7.7787
		$\hat{\vartheta}$	0.0216	0.0016	0.0459	0.0180	0.0000	0.0031	0.0016	0.0148
500	MSE	\hat{a}	0.0990	0.0003	0.0774	0.0188	0.0211	0.0030	0.0496	0.2997
		\hat{c}	0.0000	0.0001	0.0001	0.0001	0.0000	0.0017	0.1658	0.0005
		$\hat{\zeta}$	0.1729	0.0000	0.0004	0.0001	0.1656	0.0000	0.0441	0.0032
		$\hat{\psi}$	0.0000	0.0004	0.0980	0.0236	0.0000	0.0037	0.0000	0.3887
		$\hat{\vartheta}$	0.0000	0.0000	0.0006	0.0003	0.0000	0.0011	0.0001	0.0012

5.2. Tail Value at Risk (TVaR)

TVaR of X at the $100\rho\%$ security level, also named as conditional tail expectation, conditional-value at-risk, and expected shortfall and denoted by $TVaR_\rho(X)$ is the mean of all VaR values that are higher than the security threshold ρ , where $0 < \rho < 1$ [19]. That is

$$TVaR_\rho(X) = \frac{\int_\rho^1 VaR_u(X) du}{1 - \rho}.$$

Let X follow the KAP-Lomax distributions with parameters a, c, ζ, ψ and ϑ , then the TVaR of the KAP-Lomax is given by

$$TVaR_\rho(X) = \frac{1}{1 - \rho} \int_\rho^1 \frac{1}{\zeta} \left\{ \left(\frac{\log(a)}{\log(a) - \log(1 + (a - 1)[1 - (1 - u)^{\frac{1}{c}}]^{\frac{1}{\psi}})} \right)^{\frac{1}{\vartheta}} \right\} du, \tag{32}$$

Table 3. AB of KAP-Lomax for two combinations of parameters.

		$a = 1.2, c = .4, \varsigma = .7, \psi = .1, \vartheta = .8$				$a = 1.3, c = .2, \varsigma = .9, \psi = .1, \vartheta = .3$				
n	Par.	MLE	LSE	WLSE	CVME	MLE	LSE	WLSE	CVME	
25	AB	\hat{a}	4.3913	5.0591	6.4154	0.2260	1.8861	6.4474	0.0880	0.3471
		\hat{c}	0.0143	0.1945	0.2972	0.2678	0.1289	0.1502	3.8434	0.1642
		$\hat{\varsigma}$	6.6618	0.3863	0.5107	0.1551	6.7628	0.6753	0.4394	0.4247
		$\hat{\psi}$	0.0291	5.7221	7.2162	5.1177	0.1749	7.4368	0.0771	7.9491
		$\hat{\vartheta}$	0.1667	0.3966	0.5908	0.0252	0.0988	0.2255	0.1986	0.2089
50	AB	\hat{a}	2.9055	3.0936	4.9543	0.3028	1.2261	5.0452	0.3151	0.4479
		\hat{c}	0.0443	0.1286	0.2243	0.1996	0.0484	0.1240	3.1270	0.1396
		$\hat{\varsigma}$	4.9584	0.2394	0.3902	0.2516	5.7633	0.5215	0.2788	0.4319
		$\hat{\psi}$	0.0088	3.4835	5.5736	3.0047	0.0597	5.7404	0.0608	5.2087
		$\hat{\vartheta}$	0.1610	0.2582	0.4466	0.3425	0.0636	0.1863	0.0977	0.1005
100	AB	\hat{a}	1.5019	0.3077	2.6488	0.3911	0.6483	1.9943	0.2573	0.6049
		\hat{c}	0.0328	0.1029	0.1195	0.1190	0.0143	0.0950	1.7971	0.0982
		$\hat{\varsigma}$	2.7058	0.0357	0.2099	0.0192	4.0818	0.2071	0.1458	0.3040
		$\hat{\psi}$	0.0034	0.3370	2.9798	1.5783	0.0205	2.2657	0.0340	3.3466
		$\hat{\vartheta}$	0.0771	0.0507	0.2400	0.0134	0.0301	0.0984	0.0424	0.0920
200	AB	\hat{a}	0.3290	0.0281	0.6336	0.1990	0.0544	0.2898	0.2019	0.4672
		\hat{c}	0.0087	0.0304	0.0287	0.0321	0.0003	0.0467	0.7061	0.0451
		$\hat{\varsigma}$	0.6324	0.0063	0.0503	0.0262	0.2456	0.0306	0.0613	0.1173
		$\hat{\psi}$	0.0004	0.0280	0.7128	0.3946	0.0009	0.3283	0.0133	1.2942
		$\hat{\vartheta}$	0.0186	0.0109	0.0575	0.0349	0.0004	0.0061	0.0103	0.0590
500	AB	\hat{a}	0.0134	0.0006	0.0088	0.0043	0.0059	0.0116	0.0087	0.0713
		\hat{c}	0.0002	0.0003	0.0003	0.0003	0.0000	0.0089	0.0338	0.0029
		$\hat{\varsigma}$	0.0186	0.0001	0.0006	0.0003	0.0182	0.0014	0.0123	0.0074
		$\hat{\psi}$	0.0000	0.0006	0.0099	0.0048	0.0001	0.0128	0.0006	0.0812
		$\hat{\vartheta}$	0.0002	0.0002	0.0007	0.0005	0.0000	0.0072	0.0000	0.0046

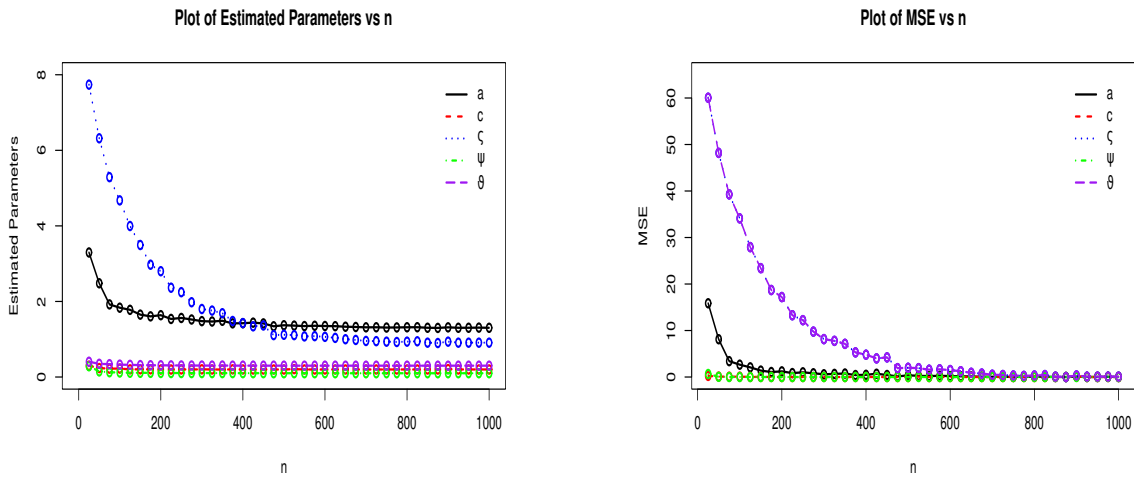
where $0 < \rho < 1$, $a, c, \varsigma, \psi, \vartheta > 0$ and $a \neq 1$.

Alternatively, using the PDF of KAP-Lomax distribution, we can derive $TVaR_\rho(X)$ as follows

$$\begin{aligned}
 TVaR_\rho(X) &= \frac{1}{1-\rho} \int_{VaR_\rho}^{\infty} x g(x) dx = \frac{1}{1-\rho} \int_{VaR_\rho}^{\infty} x \left[\sum_{b=0}^{\infty} \sum_{\ell=0}^{\infty} v_{b,\ell}(\Pi, 1) d_\ell(x, a, \varsigma, \vartheta, 1) \right] dx \\
 &= \sum_{b=0}^{\infty} \sum_{\ell=0}^{\infty} v_{b,\ell}(\Pi, 1) \frac{1}{1-\rho} \int_{VaR_\rho}^{\infty} x d_\ell(x, a, \varsigma, \vartheta, 1) dx.
 \end{aligned}$$

We have

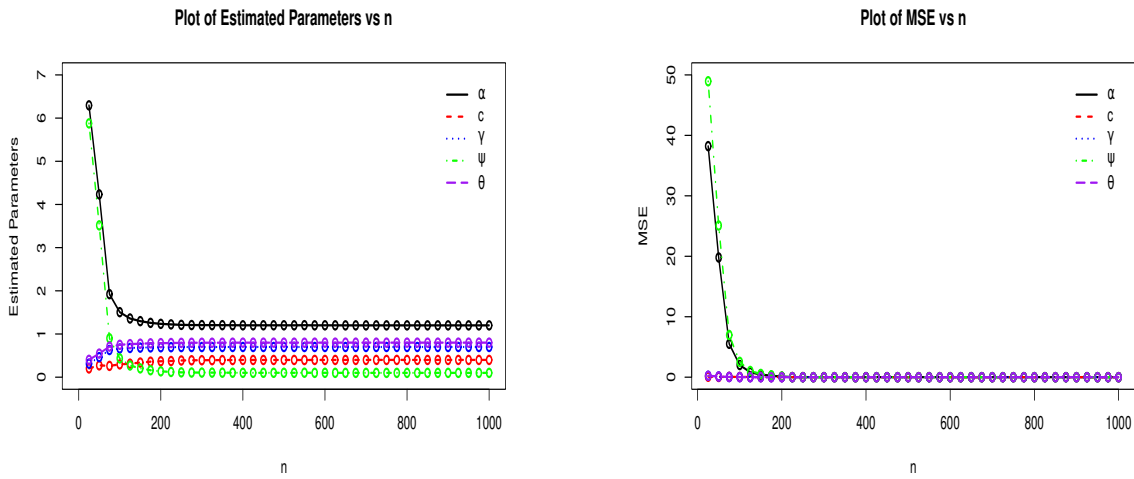
$$\int_{VaR_\rho}^{\infty} x d_\ell(x, a, \varsigma, \vartheta, 1) dx = \int_{VaR_\rho}^{\infty} x (1 + \varsigma x)^{-(\vartheta+1)} a^{(\ell+1)[1-(1+\varsigma x)^{-\vartheta}]} dx.$$



6(a) MLEs plots

6(b) MSEs plots for MLE

Figure 6. Plots of MLEs and MSEs of the KAP-Lomax for $a = 1.3, c = 0.2, \zeta = 0.9, \psi = 0.1, \vartheta = 0.3$.



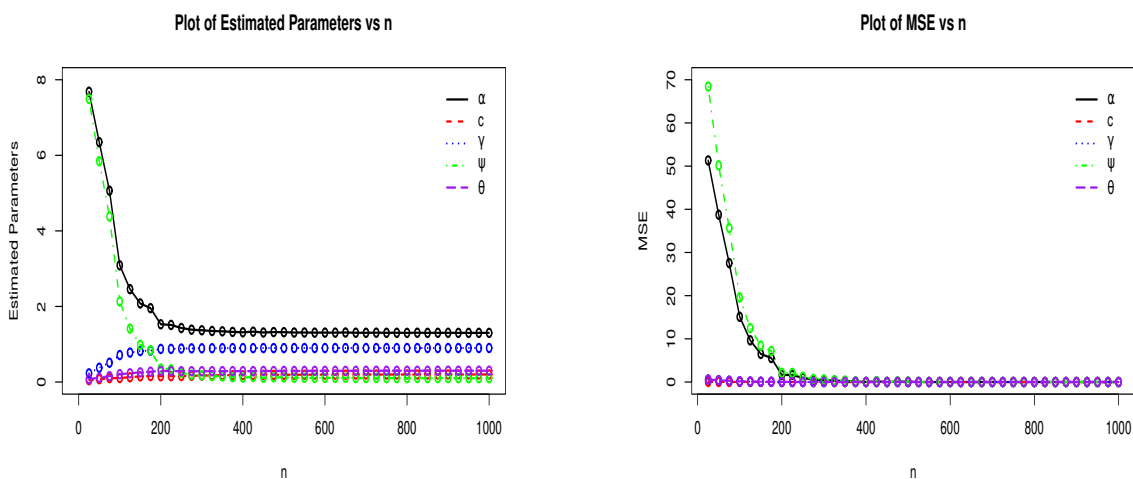
7(a) LSEs plots

7(b) MSEs plots for LSE

Figure 7. Plots of LSEs and MSEs of the KAP-Lomax for $a = 1.2, c = 0.4, \zeta = 0.7, \psi = 0.1, \vartheta = 0.8$.

Putting $y = (1 + \zeta x)^{-\vartheta}$, $x = \frac{1}{\zeta}(y^{-\frac{1}{\vartheta}} - 1)$ and $\partial x = \frac{-1}{\zeta \vartheta y^{\frac{1}{\vartheta} + 1}} \partial y$,
 where $0 < y < (1 + \zeta VaR_\rho)^{-\vartheta}$, it follows that

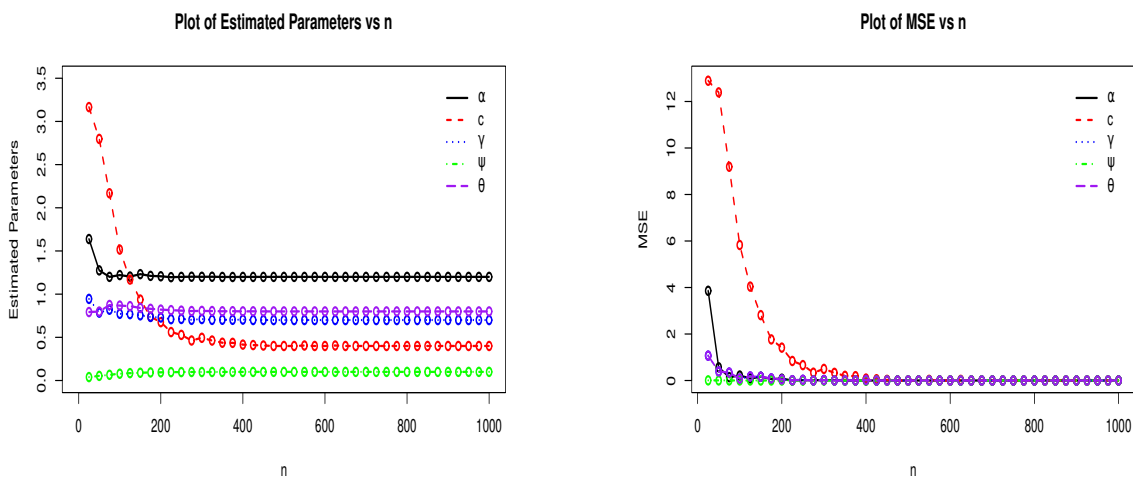
$$\int_{VaR_\rho}^{\infty} x (1 + \zeta x)^{-(\vartheta+1)} a^{(\ell+1)[1-(1+\zeta x)^{-\vartheta}]} dx = \frac{-a^{\ell+1}}{\vartheta \zeta^2} \int_0^{(1+\zeta VaR_\rho)^{-\vartheta}} \frac{(y^{\frac{1}{\vartheta}} - 1)}{a^{y^{(\ell+1)}}} \partial y.$$



8(a) LSEs plots

8(b) MSEs plots for LSE

Figure 8. Plots of LSEs and MSEs of the KAP-Lomax for $a = 1.3, c = 0.2, \varsigma = 0.9, \psi = 0.1, \vartheta = 0.3$.



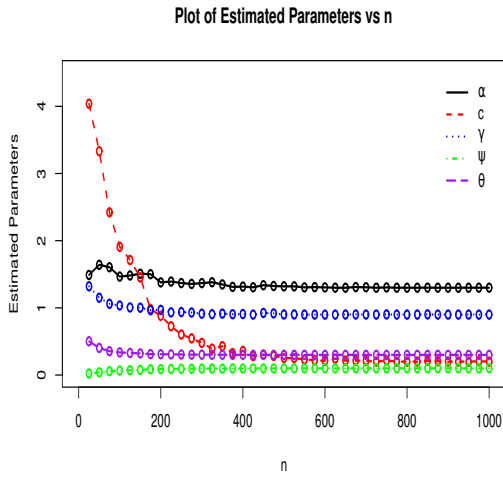
9(a) WLSEs plots

9(b) MSEs plots for WLSE

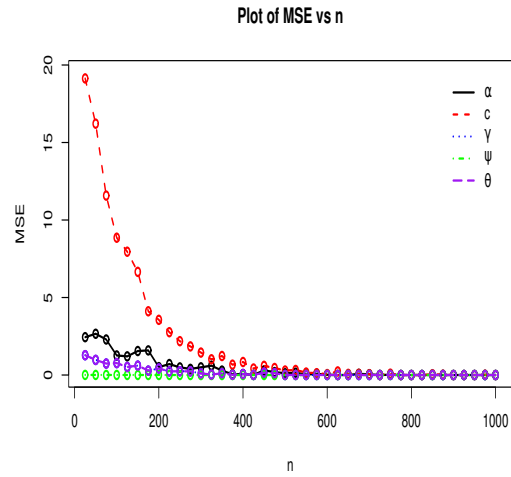
Figure 9. Plots of WLSEs and MSEs of the KAP-Lomax for $a = 1.2, c = 0.4, \varsigma = 0.7, \psi = 0.1, \vartheta = 0.8$.

Using $a^z = \sum_{k=0}^{\infty} \frac{(\log(a))^k}{k!} Z^k$, the above expression is equal to

$$\begin{aligned} & \frac{-a^{\ell+1}}{\vartheta \varsigma^2} \sum_{k=0}^{\infty} \frac{(\log(a))^k}{k!} (\ell + 1)^k \int_0^{(1+\varsigma VaR_{\rho})^{-\vartheta}} \frac{(y^{\frac{1}{\vartheta}} - 1)}{y^k} \partial y. \\ & = \frac{-a^{\ell+1}}{\vartheta \varsigma^2} \sum_{k=0}^{\infty} \frac{(\log(a))^k}{k!} (\ell + 1)^k \frac{((\varsigma VaR_{\rho} + 1)^{-\vartheta})^{1-k} \left(\vartheta(k-1) \left(((\varsigma VaR_{\rho} + 1)^{-\vartheta})^{1/\vartheta} - 1 \right) + 1 \right)}{(k-1)(\vartheta(k-1) - 1)}. \end{aligned}$$

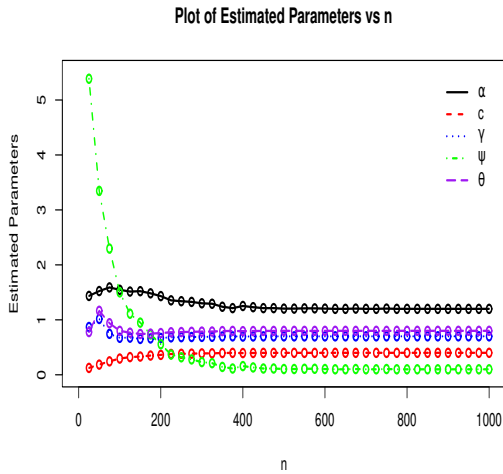


10(a) WLSEs plots

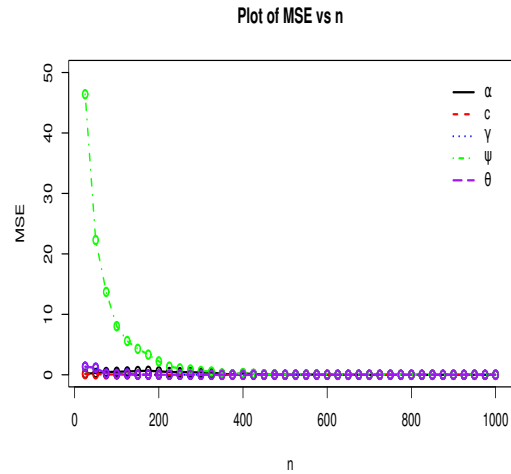


10(b) MSEs plots for WLSE

Figure 10. Plots of WLSEs and MSEs of the KAP-Lomax for $a = 1.3, c = 0.2, \zeta = 0.9, \psi = 0.1, \vartheta = 0.3$.



11(a) CVMEs plots



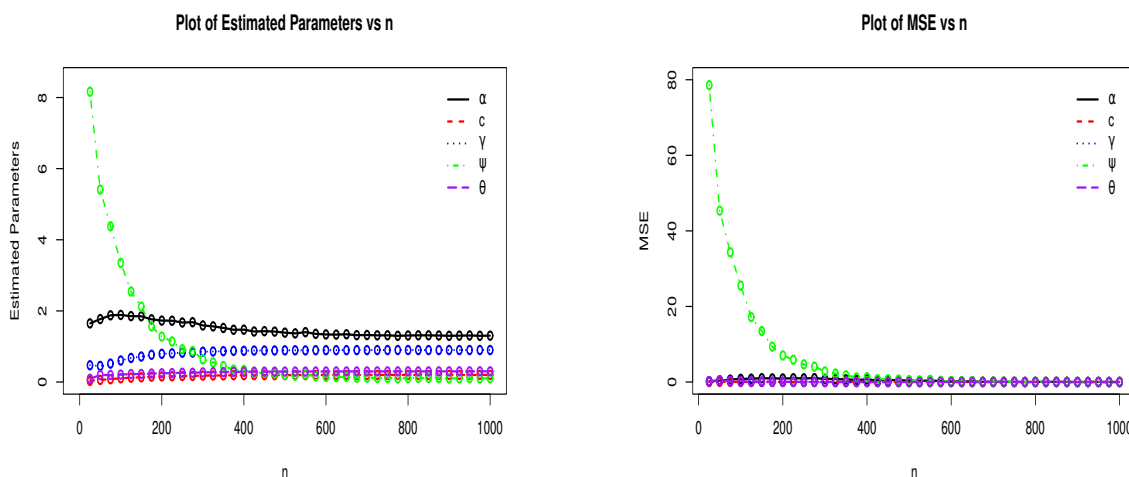
11(b) MSEs plots for CVME

Figure 11. Plots of CVMEs and MSEs of the KAP-Lomax for $a = 1.2, c = 0.4, \zeta = 0.7, \psi = 0.1, \vartheta = 0.8$.

Finally, we get

$$TVaR_p(X) = \sum_{b=0}^{\infty} \sum_{\ell=0}^{\infty} \sum_{k=0}^{\infty} v_{b,\ell}(\Pi, 1) \frac{1}{1-\rho} \frac{-a^{\ell+1}}{\vartheta \zeta^2} \frac{(\log(a))^k}{k!} (\ell+1)^k$$

$$\frac{((\zeta VaR_p + 1)^{-\vartheta})^{1-k} \left(\vartheta(k-1) \left(((\zeta VaR_p + 1)^{-\vartheta})^{1/\vartheta} - 1 \right) + 1 \right)}{(k-1)(\vartheta(k-1) - 1)}.$$



12(a) CVMEs plots

12(b) MSEs plots for CVME

Figure 12. Plots of CVMEs and MSEs of the KAP-Lomax for $a = 1.3, c = 0.2, \zeta = 0.9, \psi = 0.1, \vartheta = 0.3$.

6. Practical Illustration of the Proposed Model

We illustrate a new heavy-tailed distribution by analyzing four real data sets with one of its special models (KAP-Lomax).

Data set 1: Home insurance data (Theft data Nagarjuna et al. [17]) represents the 120 theft claims made in a home insurance portfolio.

Data set 2: Unemployment insurance data set represents monthly metrics on unemployment insurance from July 2008 to April 2013, including 58 observations, as reported by the Department of Labor, Licensing and Regulation, State of Maryland, USA, which was primarily used by Afify et al. [18]. There are 21 variables in the data, and we focus on analyzing variable number 12. The data are available at: <https://catalog.data.gov/dataset/unemployment-insurance-data-july-2008-to-april-2013>.

Data set 3: Strength data represent measures for 69 single-carbon fibers (and impregnated 1000-carbon fiber tows) Bader and Priest [35].

Data set 4: GDP growth data of 31 observations for GDP growth (% per year) of Egypt discussed by [36].

KAP-Lomax distribution is compared with some other well-known distributions, including Kum-G power Lomax (KPL) [17], alpha power Lomax (APL) [20], Marshall-Olkin alpha power Lomax (MOAPL) [3], Kum alpha power inverted exponential (KAPIE) [2], Kum-G power Weibull (KGPW) [31], Kum modified inverse Weibull (KMIW) [32], Marshall-Olkin alpha power inverse Weibull (MOAPIW) [33], alpha power inverse Weibull (APIW) [23] and Kum exponentiated inverse Rayleigh (KEIR) [34]. The following are the rival distributions' CDFs:

(1) KPL Distribution

$$G(x) = 1 - \left[1 - \left(1 - \left(\frac{\lambda}{\lambda + x^\beta} \right)^\alpha \right)^\psi \right]^c, \quad x > 0, a, \beta, c, \lambda, \psi > 0. \tag{33}$$

(2) APL Distribution

$$G(x) = \frac{a^{1 - \left(1 + \frac{x}{\lambda}\right)^{-\beta}} - 1}{a - 1}, \quad x > 0, a, \beta, \lambda > 0. \tag{34}$$

(3) MOAPL Distribution

$$G(x) = \frac{a^{1-(1+\frac{x}{\lambda})^{-\beta}} - 1}{(a-1)\left(\vartheta + \frac{(1-\vartheta)}{(a-1)}\left(a^{1-(1+\frac{x}{\lambda})^{-\beta}} - 1\right)\right)}, \quad x > 0, a, \beta, \lambda, \vartheta > 0. \tag{35}$$

(4) KAPIE Distribution

$$G(x) = 1 - \left[1 - \left(\frac{a^{e^{-\frac{\lambda}{x}}} - 1}{a-1}\right)^\psi\right]^c, \quad x > 0, a, c, \lambda, \psi > 0, a \neq 1. \tag{36}$$

(5) KGPW Distribution

$$G(x) = 1 - [1 - (1 - e^{(1-(1+\frac{x}{\lambda})^\vartheta)})^\varsigma]^c, \quad x > 0, \varsigma, c, a, \lambda, \vartheta > 0. \tag{37}$$

(6) KMIW Distribution

$$G(x) = 1 - [1 - e^{-\beta(\frac{\lambda}{x} + \frac{\vartheta}{x^\alpha})}]^c, \quad x > 0, \beta, c, a, \lambda, \vartheta > 0. \tag{38}$$

(7) MOAPIW Distribution

$$G(x) = \frac{(a^{e^{-\lambda x^{-\beta}}} - 1)}{(a-1)\vartheta - (\vartheta-1)(a^{e^{-\lambda x^{-\beta}}} - 1)}, \quad x > 0, a, \beta, \lambda, \vartheta > 0. \tag{39}$$

(8) APIW Distribution

$$G(x) = \frac{a^{e^{-\lambda x^{-\beta}}} - 1}{(a-1)}, \quad x > 0, a, \beta, \lambda > 0, a \neq 1. \tag{40}$$

(9) KEIR Distribution

$$G(x) = 1 - [1 - (e^{-\frac{\vartheta}{x^2}})^{\varsigma a}]^\beta, \quad x > 0, \varsigma, \beta, a, \vartheta > 0. \tag{41}$$

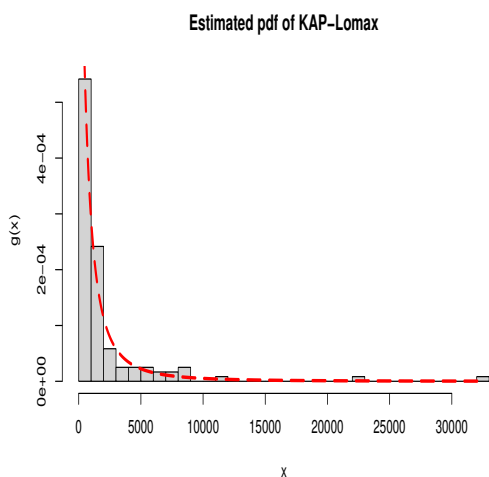
Some commonly used analytical measures called the Akaike Information Criterion ($AIC = 2k - 2l$), Bayesian Information Criterion ($BIC = k \log(n) - 2l$), and consistent Akaike information criterion ($CAIC = \frac{2nk}{n-k-1} - 2l$) have been considered to decide which distribution fits the data better. Here l is the log-likelihood function assessed at MLEs, n denotes the sample size, and k denotes the number of model parameters. The statistics Cramer-von Mises (W), Anderson-Darling (A) and Kolmogorov Smirnov (KS) with corresponding p-values (p) are also applied for testing goodness of fit.

In the practical illustration of the proposed model, Tables 4 and 5 show the MLEs of the model parameters, whereas Tables 6 and 7 give the analytical measures of the competing models for all data sets. The results reported that the KAP-Lomax distribution has the lowest analytical measures and highest p-values. Furthermore, the estimated PDF, CDF, and Kaplan-Meier survival plots of the KAP-Lomax model are sketched in Figures (13-18) for the four data sets. The plots in the figures confirm the close fitting of the KAP-Lomax. The goodness of fit tests and all the criteria of model selection indicate that the KAP-Lomax beats all other models for all data sets.

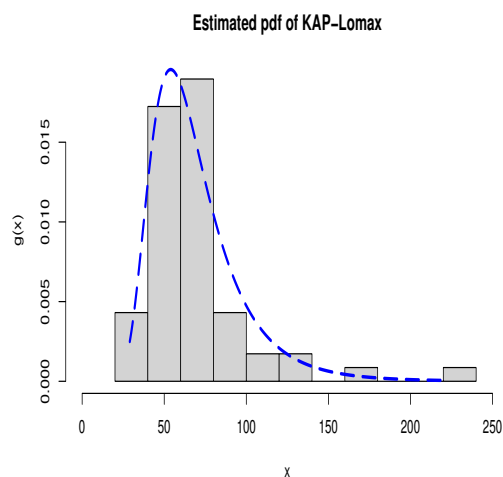
It is evident that while modeling data, a model becomes heavier-tailed as its risk value rises. We have computed the VaR and TVaR measures of the KAP-Lomax, KGPW, KMPLo, and NEHTW distributions using the estimated parameter values of data sets 1 and 2. The numerical results are reported in Tables 8 and 9 and displayed graphically in Figures 19 and 20. A model with higher risk measure values is said to have a heavy tail. From the numerical values for the actuarial measures (VaR and TVaR) of the proposed model and other heavy-tailed distributions provided in Tables 8 and 9, it is clear that the KAP-Lomax distribution has a heavier tail than KGPW, KMPLo, and NEHTW distributions and is a good candidate for modeling heavy-tailed insurance data sets.

Table 4. The values of the MLEs using data set 1 & data set 2.

Models	$\hat{\alpha}$	$\hat{\beta}$	\hat{c}	$\hat{\zeta}$	$\hat{\lambda}$	$\hat{\psi}$	$\hat{\vartheta}$
Data set 1							
KAP-Lomax	17.8899	-	3.8174	0.0038	-	1.1087	0.5007
KPL	2.0004	0.2402	13.8810	-	6.5333	7.8513	-
KGPW	0.3573	-	4.0192	6.1828	6.8133	-	0.4594
MOAPL	9.0375	1.0022	-	-	14.2705	-	19.8844
KMIW	0.3352	3.9199	5.4181	-	2.4977	-	4.9520
MOAPIW	8.8117	0.9227	-	-	14.6178	-	11.4620
APIW	17.0288	0.6817	-	-	21.2967	-	-
KAPIE	160.533	-	0.6611	-	93.2676	0.5281	-
APL	19.9285	0.5102	-	-	22.0490	-	-
KEIR	7.9914	0.1188	-	5.7977	-	-	0.2247
Data set 2							
KAP-Lomax	12.8144	-	1.6655	0.0299	-	20.0383	3.6878
KPL	1.2330	0.9388	9.0901	-	12.0027	17.9278	-
KGPW	1.4404	-	2.4876	10.0530	11.1282	-	0.4215
MOAPL	20.6517	4.4780	-	-	39.1408	-	19.3499
KMIW	0.9158	11.3262	12.9967	-	2.5875	-	10.0618
MOAPIW	14.4257	1.8008	-	-	19.9610	-	24.2016
APIW	15.6162	1.0901	-	-	21.9568	-	-
KAPIE	13.6907	-	13.2632	-	4.5774	15.5154	-
APL	17.4612	1.7587	-	-	37.1871	-	-
KEIR	7.9004	2.2513	-	22.1024	-	-	29.4476



13(a) Estimated PDF for data set 1

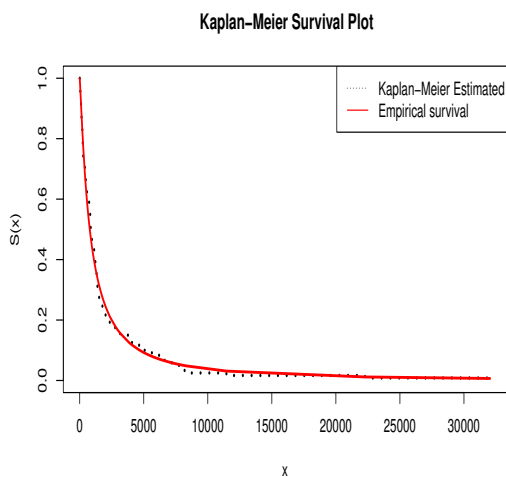


13(b) Estimated PDF for data set 2

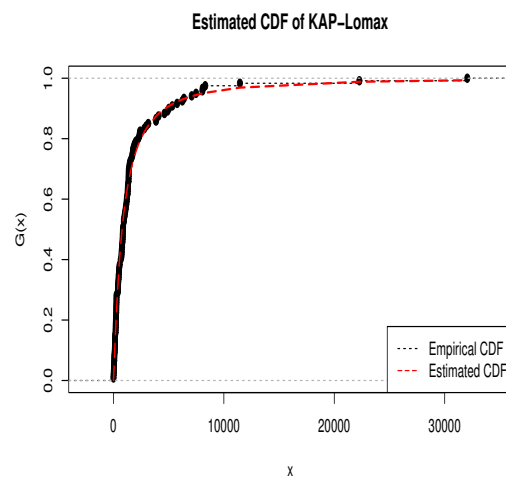
Figure 13. Estimated PDFs of KAP-Lomax distribution for data sets 1 and 2.

Table 5. The values of the MLEs using data set 3 & data set 4.

Models	\hat{a}	$\hat{\beta}$	\hat{c}	$\hat{\zeta}$	$\hat{\lambda}$	$\hat{\psi}$	$\hat{\vartheta}$
Data set 3							
KAP-Lomax	14.8212	-	8.0254	0.1124	-	2.6468	7.9480
KPL	2.5731	2.2131	5.1902	-	6.2256	1.5795	-
KGPW	3.9477	-	4.0079	0.6661	4.5197	-	6.0166
MOAPL	5.8668	15.1809	-	-	4.6536	-	24.0247
KMIW	0.8147	1.4510	7.5829	-	1.4567	-	3.5133
MOAPIW	11.5529	1.5259	-	-	0.0593	-	8.1716
APIW	14.3146	1.0787	-	-	0.3446	-	-
KAPIE	18.9568	-	4.4446	-	0.1803	4.4533	-
APL	20.9860	14.4032	-	-	10.4985	-	-
KEIR	4.7436	0.2069	-	0.0772	-	-	0.0382
Data set 4							
KAP-Lomax	5.2636	-	2.9968	0.1112	-	4.9699	4.3846
KPL	3.1411	0.9235	4.2784	-	6.7270	7.8441	-
KGPW	1.0421	-	0.6819	3.5336	14.2816	-	4.0034
MOAPL	12.5092	10.3995	-	-	10.2503	-	19.1395
KMIW	1.5412	2.4521	0.6086	-	1.3379	-	4.6857
MOAPIW	9.6277	3.0459	-	-	4.2696	-	9.3924
APIW	20.7758	2.2517	-	-	7.1376	-	-
KAPIE	15.7300	-	7.4319	-	0.2571	14.2067	-
APL	13.3608	9.0779	-	-	23.7491	-	-
KEIR	1.9570	1.1229	-	1.8186	-	-	3.7978



14(a) Kaplan-Meier survival plot

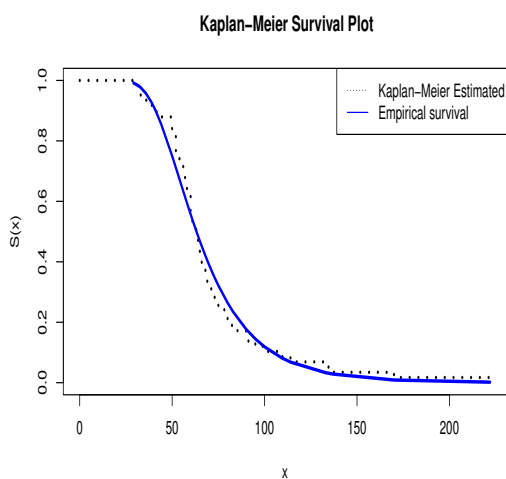


14(b) Estimated CDF plot

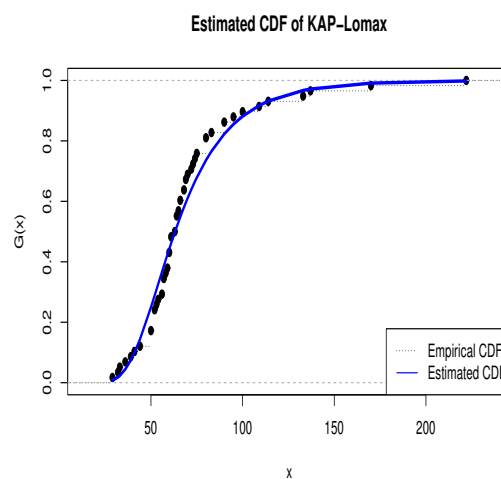
Figure 14. Kaplan-Meier survival and Estimated CDF of KAP-Lomax for data set 1.

Table 6. Analytical measures of KAP-Lomax and other competitive using data set 1 & data set 2.

Models	$-2l(\cdot)$	AIC	BIC	CAIC	W	A	KS	p
Data set 1								
KAP-Lomax	1012.395	2034.789	2048.727	2035.316	0.08043	0.40371	0.06063	0.7697
KPL	1012.631	2035.262	2049.200	2035.788	0.08567	0.44812	0.06067	0.7690
KGPW	1012.986	2035.972	2049.91	2036.498	0.09499	0.48340	0.06629	0.6673
MOAPL	1015.969	2039.938	2051.088	2040.286	38.3380	232.6436	0.83409	2.2e-16
KMIW	1016.36	2042.72	2056.658	2043.247	0.17470	0.90859	0.11221	0.0974
MOAPIW	1019.088	2046.177	2057.327	2046.524	0.17349	0.92550	0.10439	0.1462
APIW	1027.855	2061.71	2070.072	2061.917	0.35811	2.00469	0.11659	0.07661
KAPIE	1033.676	2075.351	2086.501	2075.699	0.49956	2.85248	0.19207	0.00028
APL	1042.307	2090.613	2098.976	2090.82	0.29323	1.58075	0.20065	0.00012
KEIR	1099.913	2207.826	2218.976	2208.174	1.58132	9.23647	0.3402	1.728e-12
Data set 2								
KAP-Lomax	265.8054	541.6108	551.913	542.7647	0.14600	0.81043	0.11532	0.4235
KAPIE	268.2448	544.4895	552.7313	545.2442	0.17533	0.97139	0.12332	0.341
KEIR	268.7409	545.4817	553.7235	546.2364	0.20700	1.18970	0.1422	0.1914
KGPW	267.9163	545.8326	556.1348	546.9864	0.21648	1.17109	0.23894	0.0026
KMIW	267.9986	545.9973	556.2995	547.1511	0.20439	1.10553	0.13118	0.271
KPL	268.9099	547.8198	558.122	548.9736	0.20719	1.12167	0.11719	0.4032
MOAPL	278.002	564.004	572.2457	564.7587	18.15555	114.6945	0.96342	2.2e-16
MOAPIW	295.1993	598.3986	606.6404	599.1533	0.17771	0.96570	0.32781	7.714e-06
APL	306.882	619.764	625.9454	620.2085	0.19814	1.07392	0.35934	6.252e-07
APIW	309.1480	624.2959	630.4773	624.7404	0.16909	0.92228	0.32585	8.951e-06



15(a) Kaplan-Meier survival plot

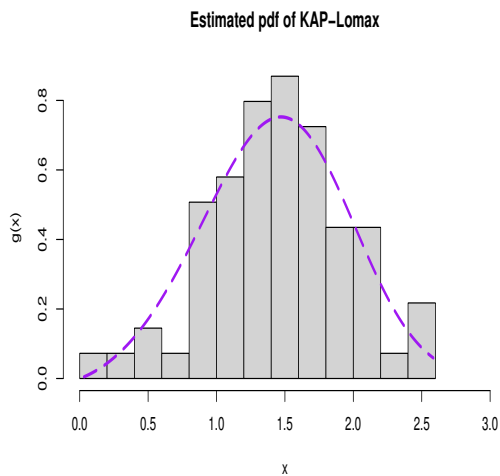


15(b) Estimated CDF plot

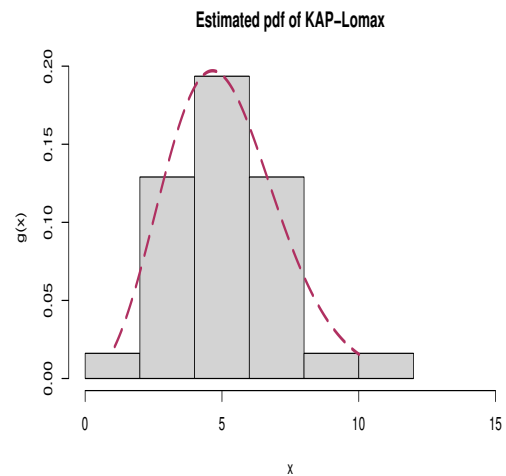
Figure 15. Kaplan-Meier survival and Estimated CDF of KAP-Lomax for data set 2.

Table 7. Analytical measures of KAP-Lomax and other competitive using data set 3 & data set 4.

Models	$-2l(\cdot)$	AIC	BIC	CAIC	W	A	KS	p
Data set 3								
KAP-Lomax	54.701	119.402	130.573	120.355	0.1033	0.7267	0.0771	0.8054
KPL	56.107	122.214	133.384	123.166	0.1237	0.8646	0.0814	0.7493
KGPW	59.303	127.607	138.778	128.56	0.1831	0.9103	0.0826	0.6333
MOAPL	61.201	129.112	142.542	131.235	0.2105	0.9314	0.0907	0.5492
KMIW	78.814	167.628	178.799	168.581	0.6518	3.9757	0.1817	0.02099
MOAPIW	100.208	208.416	217.353	209.041	1.2004	6.9448	0.2828	3.198e-05
APIW	110.753	227.506	234.208	227.875	1.5395	8.6172	0.2863	2.439e-05
KAPIE	90.827	189.654	198.590	190.279	1.0482	6.1159	0.2158	0.003229
APL	74.703	155.407	162.109	155.776	0.19628	1.3044	0.2692	9.04e-05
KEIR	160.468	328.937	337.873	329.562	3.0225	15.5482	0.4756	5.489e-14
Data set 4								
KAP-Lomax	66.212	142.424	149.594	144.824	0.0248	0.2007	0.0543	0.9999
KAPIE	68.753	145.506	151.242	147.044	0.0804	0.5707	0.1214	0.7052
KEIR	74.936	157.873	163.609	159.412	0.2435	1.5741	0.2044	0.1296
KGPW	66.502	143.172	151.178	146.814	0.0415	0.2618	0.0916	0.9742
KMIW	67.892	145.785	152.955	148.185	0.1255	0.8404	0.1520	0.4282
KPL	66.426	142.852	150.022	145.252	0.0306	0.2414	0.0806	0.9778
MOAPL	67.102	145.665	153.163	147.894	0.0568	0.2869	0.1324	3.331e-16
MOAPIW	68.743	145.486	151.222	147.025	0.0735	0.5362	0.1258	0.6643
APL	75.051	156.102	160.404	156.991	0.0187	0.1608	0.2491	0.03502
APIW	71.417	148.834	153.136	149.723	0.1408	0.9459	0.1496	0.4482

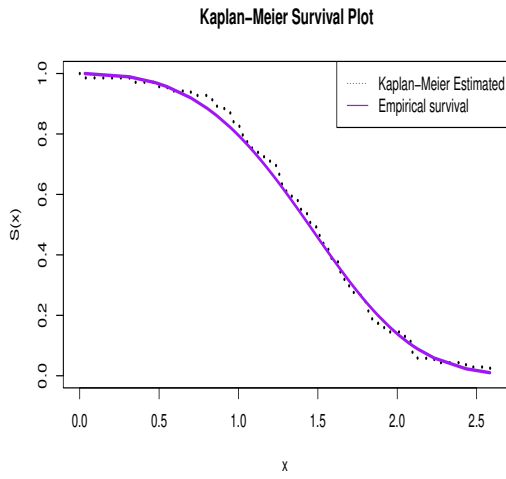


16(a) Estimated PDF for data set 3

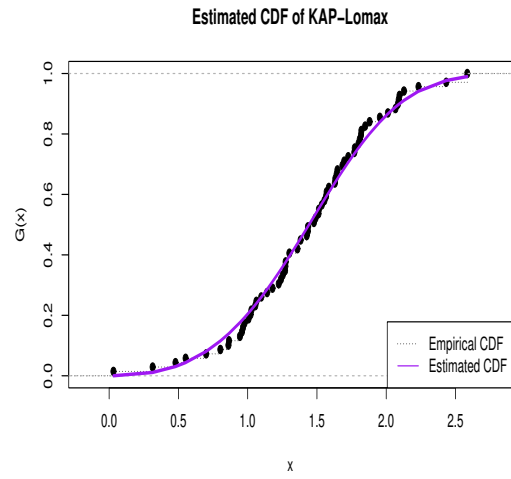


16(b) Estimated PDF for data set 4

Figure 16. Estimated PDFs of KAP-Lomax distribution for data sets 3 and 4.

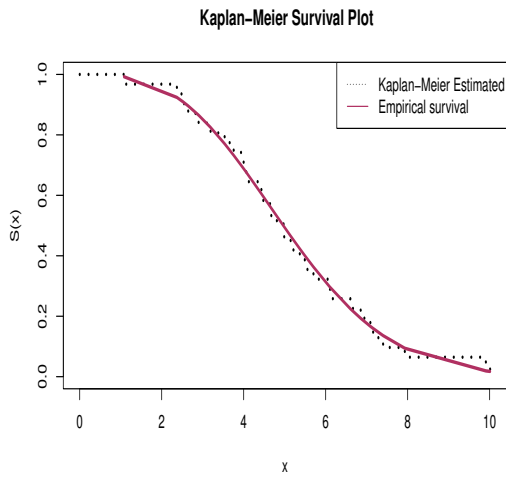


17(a) Kaplan-Meier survival plot

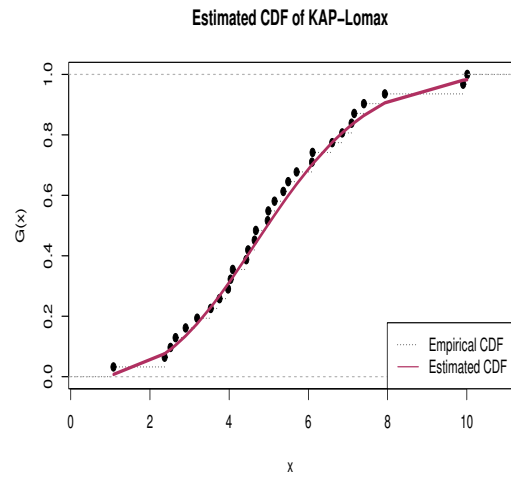


17(b) Estimated CDF plot

Figure 17. Kaplan-Meier survival and Estimated CDF of KAP-Lomax for data set 3.



18(a) Kaplan-Meier survival plot



18(b) Estimated CDF plot

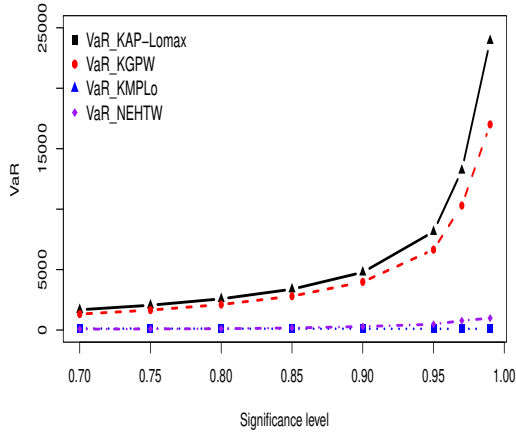
Figure 18. Kaplan-Meier survival and Estimated CDF of KAP-Lomax for data set 4.

Table 8. Results for the actuarial measures for data set 1.

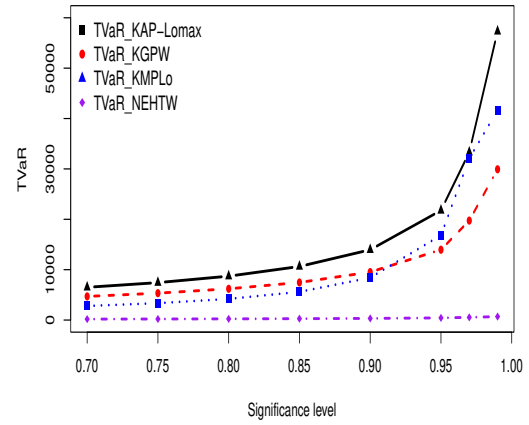
Models	Par.	Level of sig	VaR	TVaR
KAP-Lomax	$\hat{a} = 17.8899$.700	1677.057	6501.807
	$\hat{c} = 3.8174$.750	2054.646	7430.88
	$\hat{\zeta} = 0.0038$.800	2580.921	8713.156
	$\hat{\psi} = 1.1087$.850	3378.910	10634.58
	$\hat{\vartheta} = 0.5007$.900	4776.742	13951.08
		.950	8133.276	21754.62
		.975	13201.138	33301.71
	.990	23929.533	57303.88	
KGPW	$\hat{\zeta} = 5.5622$.700	1321.159	4692.764
	$\hat{c} = 4.0192$.750	1651.513	5335.712
	$\hat{a} = 0.3573$.800	6202.705	5547.104
	$\hat{\lambda} = 6.8133$.850	2802.546	7459.937
	$\hat{\vartheta} = 0.4594$.900	3982.853	9524.003
		.950	6648.923	13957.72
		.975	10297.091	19741.01
	.990	17003.221	29927.28	
KMPLo	$\hat{\alpha} = 0.7442$.700	128.2814	2791.397
	$\hat{\beta} = 0.5597$.750	122.5606	3353.100
	$\hat{\lambda} = 28.2418$.800	117.2805	4195.351
		.850	112.3947	5598.733
		.900	107.8632	8404.996
		.950	103.6507	16822.87
		.975	101.6544	32057.99
	.990	100.4897	41672.88	
NEHTW	$\hat{\alpha} = 0.7181$.700	74.51406	189.0991
	$\hat{\beta} = 7.4567$.750	91.49947	210.3863
	$\hat{\theta} = 0.0052$.800	113.62808	237.4741
		.850	174.14560	273.9729
		.900	290.59615	328.2158
		.950	478.23049	427.849
		.975	774.97520	535.3441
	.990	985.08940	688.2603	

Table 9. Results for the actuarial measures for data set 2.

Models	Par.	Level of sig	VaR	TVaR
KAP-Lomax	$\hat{a} = 17.8899$.700	77.60296	104.5675
	$\hat{c} = 3.8174$.750	82.24932	109.5091
	$\hat{\zeta} = 0.0038$.800	87.90038	115.6437
	$\hat{\psi} = 1.1087$.850	95.20923	123.7334
	$\hat{\vartheta} = 0.5007$.900	105.69642	135.5623
		.950	124.51739	157.2066
		.975	144.91706	181.0136
	.990	175.01004	216.4705	
KGPW	$\hat{\zeta} = 5.5622$.700	80.24081	104.3642
	$\hat{c} = 4.0192$.750	84.97115	108.7274
	$\hat{a} = 0.3573$.800	90.56114	113.9897
	$\hat{\lambda} = 6.8133$.850	97.53779	120.6862
	$\hat{\vartheta} = 0.4594$.900	107.08347	130.0237
		.950	122.99248	145.893
		.975	138.72625	161.8248
	.990	159.62274	183.1913	
KMPLo	$\hat{\alpha} = 0.7235$.700	13.94220	58.46644
	$\hat{\beta} = 0.9156$.750	14.03639	70.09191
	$\hat{\lambda} = 32.3267$.800	14.19679	87.4700
		.850	14.53106	106.2412
		.900	14.88462	116.2214
		.950	15.25918	123.7864
		.975	15.65672	135.7659
	.990	16.07942	152.7621	
NEHTW	$\hat{\alpha} = 0.0041$.700	13.62591	18.39873
	$\hat{\beta} = 20.8835$.750	14.68742	19.24919
	$\hat{\theta} = 41.5084$.800	15.90025	20.24189
		.850	17.35183	21.45562
		.900	19.23105	23.06224
		.950	22.11224	25.58821
		.975	24.69207	27.90114
	.990	27.77287	30.71215	

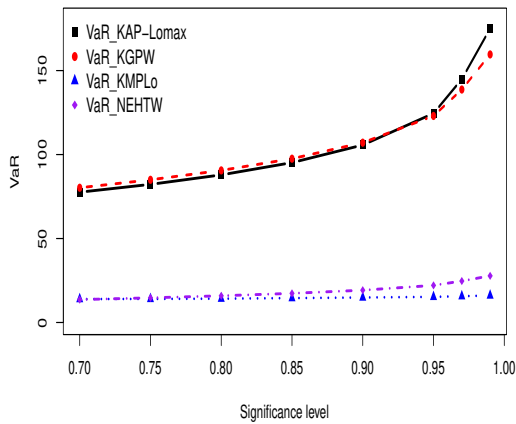


19(a) VaR plots

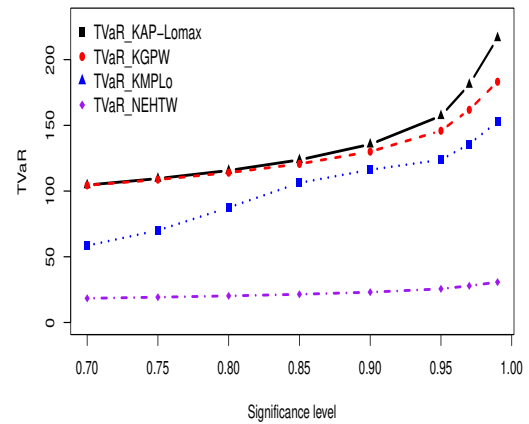


19(b) TVaR plots

Figure 19. Graphical sketching of VaR and TVaR for the home insurance data.



20(a) VaR



20(b) TVaR

Figure 20. Graphical sketching of VaR and TVaR for the unemployment insurance data.

7. Conclusion

In this paper, a KAPT family has been introduced. Introducing the new family aims to improve the distributional flexibility of the fundamental/modified distributions for modeling data. The modified version of the Lomax model, the KAP-Lomax, is studied in depth. Four estimation methods are used to estimate the KAP-Lomax model parameters. The performance of the estimates is assessed using a simulation study. Four real data sets related to insurance, finance, and reliability have been analyzed. The heavy-tailed characteristics of the KAP-Lomax using KGPW, KMPLo, and NEHTW distributions are examined through actuarial measures for data sets 1 and 2. The Wolfram Mathematica software version 12.0 and packages such as AdequacyModel, rootSolve, uniroot, optim, nlm, nlminb, L-BFGS-B, ggplot2 from R software are used for numerical implementation. The performance of KAP-Lomax has been compared with nine other well-known competitors. The behavior of the tail using actuarial measures shows that the KAP-Lomax outperforms. The proposed method is recommended to have extensive applications in the actuarial sciences, insurance industries, financial sectors, reliability, and other related areas. The suggested family is also expected to be an addition to the construction of widely applicable probability models.

Acknowledgement

The authors would like to thank the reviewers and the editor for their constructive comments and suggestions during the review process.

REFERENCES

1. P. Kumaraswamy, *A generalized probability density function for double-bounded random processes*, Journal of Hydrology, vol. 46, no. 2, pp. 78–88, 1980.
2. J. Thomas, S.C. Zelibe and E. Eyefia, *Kumaraswamy alpha power inverted exponential distribution: properties and applications*, Istatistik Journal of the Turkish Statistical Association, vol. 12, no. 1, pp. 35–48, 2019.
3. H. M. Almongy, E. M. Almetwally, and A. E. Mubarak, *Marshall–Olkin alpha power Lomax distribution: Estimation methods, applications on physics and economics*, Pakistan Journal of Statistics and Operation Research, vol. 17, no. 1, pp. 135–153, 2021.
4. N. Poonia and S. Azad, *Alpha power exponentiated Teissier distribution with application to climate datasets*, Theoretical and Applied Climatology, vol. 149, no. 1, pp. 339–353, 2022.
5. L.A. Baharith, *Alpha-power Kumaraswamy–Burr III distribution with applications of COVID-19 data in Saudi Arabia*, Results in Physics, vol. 35, pp. 105–353, 2022.
6. F. Ulubekova and G. Ozel, *Alpha Power-Kumaraswamy Distribution with An Application on Survival Times of Cancer Patients*, Journal of Computer Science Research, vol. 2, no. 2, pp. 1855–7771, 2020.
7. C. Adcock, M. Eling and N. Loperfido, *Skewed distributions in finance and actuarial science: a review*, The European Journal of Finance, vol. 21, no. 1, pp. 1253–1281, 2015.
8. K. Cooray and M.M. Ananda, *Modeling actuarial data with a composite lognormal-Pareto model*, Scandinavian Actuarial Journal, vol. 2005, no. 5, pp. 321–334, 2005.
9. R. Kazemi and M. Noorzadeh, *A comparison between skew-logistic and skew-normal distributions*, Matematika: Malaysian Journal of Industrial and Applied Mathematics, vol. 31, no. 1, pp. 15–24, 2015.
10. A. Punzo, L. Bagnato and A. Maruotti, *Compound unimodal distributions for insurance losses*, Insurance: Mathematics and Economics, vol. 81, no. 8, pp. 95–107, 2018.
11. R. Vernic, *Multivariate skew-normal distributions with applications in insurance*, Insurance: Mathematics and Economics, vol. 38, no. 2, pp. 413–426, 2006.
12. G. M. Cordeiro and M. de Castro, *A new family of generalized distributions*, Journal of Statistical Computation and Simulation, vol. 81, no. 7, pp. 883–898, 2011.
13. A. Mahdavi and D. Kundu, *A new method for generating distributions with an application to exponential distribution*, Communications in Statistics-Theory and Methods, vol. 46, no. 13, pp. 6543–6557, 2017.
14. K. S. Lomax, *Business failures: Another example of the analysis of failure data*, Journal of the American Statistical Association, vol. 49, no. 268, pp. 847–852, 1954.
15. J. Moors, *A quantile alternative for kurtosis*, Journal of the Royal Statistical Society: Series D (The Statistician), vol. 37, no. 1, pp. 25–32, 1988.
16. P. Artzner, *Application of coherent risk measures to capital requirements in insurance*, North American Actuarial Journal, vol. 3, no. 2, pp. 11–25, 1999.
17. V. B. Nagarjuna, R. V. Vardhan and C. Chesneau, *Kumaraswamy generalized power Lomax distribution and its applications*, Stats, vol. 4, no. 1, pp. 28–45, 2021.
18. A. Z. Afify, A. M. Gemeay and N. A. Ibrahim, *The heavy-tailed exponential distribution: risk measures, estimation, and application to actuarial data*, Mathematics, vol. 8, no. 8, pp. 1–28, 2020.
19. S. A. Klugman, H. H. Panjer and G. E. Willmot, *Loss Models: From Data to Decisions*, John Wiley & Sons, New York, 2019.

20. Y. M. Bulut, F. Z. Dogru and O. Arslan, *Alpha power Lomax distribution: Properties and application*, Journal of Reliability and Statistical Studies, vol. 14, no. 1, pp. 17–32, 2021.
21. R. A. ZeinEldin, M Ahsan ul Haq, S. Hashmi and M. Elsehety, *Alpha power transformed inverse Lomax distribution with different methods of estimation and applications*, Complexity, vol. 2020, no. 1, pp. 1–15, 2020.
22. H. S. Klakattawi, W. H. Aljuhani and L. A. Baharith, *Alpha Power Exponentiated New Weibull-Pareto Distribution: Its Properties and Applications*, Pakistan Journal of Statistics & Operation Research, vol. 18, no. 3, pp. 703–720, 2022.
23. A. M. Basheer, *Alpha power inverse Weibull distribution with reliability application*, Journal of Taibah University for Science, vol. 13, no. 1, pp. 423–432, 2019.
24. M. L. Ahmed, *On the alpha power Kumaraswamy distribution: Properties, simulation and application*, Revista Colombiana de Estadística, vol. 43, no. 2, pp. 285–313, 2020.
25. K. Bagci, N. Erdogan, T. Arslan and H. E. Celik, *Alpha power inverted Kumaraswamy distribution: Definition, different estimation methods, and application*, Pakistan Journal of Statistics and Operation Research, vol. 18, no. 1, pp. 13–25, 2022.
26. S. Al-Marzouki, F. Jamal, C. Chesneau and M. Elgarhy, *Type II Topp Leone power Lomax distribution with applications*, Mathematics, vol. 8, no. 1, pp. 1–26, 2019.
27. A. A. Ogunde, A. U. Chukwu and I. O. Oseghale, *The Kumaraswamy Generalized Inverse Lomax distribution and Applications to Reliability and survival data*, Scientific African, vol. 19, no. 5, pp. 1–15, 2022.
28. E. H. A. Rady, W. Hassanein and T. Elhaddad, *The power Lomax distribution with an application to bladder cancer data*, SpringerPlus, vol. 5, pp. 1–22, 2016.
29. A. S. Hassan and M. Abd-Allah, *On the inverse power Lomax distribution*, Annals of Data Science, vol. 6, pp. 259–278, 2019.
30. M. H. Tahir, G. M. Cordeiro, M. Mansoor and M. Zubair, *The Weibull-Lomax distribution: properties and applications*, Hacettepe Journal of Mathematics and Statistics, vol. 44, no. 2, pp. 455–474, 2015.
31. M. A. Selim and A. M. Badr, *The Kumaraswamy generalized power Weibull distribution*, Mathematical Theory and Modeling, vol. 6, pp. 110–124, 2016.
32. G. Aryal and I. Elbatal, *Kumaraswamy modified inverse Weibull distribution: Theory and application*, Applied Mathematics & Information Sciences, vol. 9, no. 2, pp. 651–660, 2015.
33. A. Basheer, E. Almetwally and H. Okasha, *Marshall-Olkin Alpha Power Inverse Weibull Distribution: Non Bayesian and Bayesian Estimations*, Journal of Statistics Applications & Probability, vol. 10, no. 2, pp. 327–345, 2020.
34. M. A. ul Haq, *Kumaraswamy exponentiated inverse Rayleigh distribution*, Mathematical Theory and Modeling, vol. 6, no. 3, pp. 93–104, 2016.
35. M. G. Bader and A. M. Priest, *Statistical Aspects of Fibre and Bundle Strength in Hybrid Composites*, Progress in science and engineering of composites, vol. 2, pp. 1129–1136, 1982.
36. E. M. Almetwally and H. M. Almongy, *Maximum product spacing and Bayesian method for parameter estimation for generalized power Weibull distribution under censoring scheme*, Journal of Data Science, vol. 17, no. 2, pp. 407–444, 2019.
37. J. Beirlant, G. Matthys and G. Dierckx, *Heavy-tailed distributions and rating*, ASTIN Bulletin: The Journal of the IAA, vol. 31, no. 1, pp. 37–58, 2001.
38. J. Zhao, Z. Ahmad, E. Mahmoudi, E. H. Hafez, M.M. Mohie and El-Din, *A new class of heavy-tailed distributions: modeling and simulating actuarial measures*, Complexity, vol. 2021, pp. 1–18, 2021.
39. N. M. Alfaer, A. M. Gemeay, H. M. Aljohani and A. Z. Afify, *The extended log-logistic distribution: inference and actuarial applications*, Mathematics, vol. 9, no. 12, pp. 1386, 2021.
40. Z. Ahmad, E. Mahmoudi and G. Hamedani, *A Class of Claim Distributions: properties, characterizations and applications to insurance claim data*, Communications in Statistics-Theory and Methods, vol. 51, no. 7, pp. 2183–2208, 2022.
41. M. Arif, D. M. Khan, S. K. Khosa, M. Aamir, A. Aslam, Z. Ahmad and W. Gao, *Modelling Insurance Losses with a New Family of Heavy-Tailed Distributions*, Computers, Materials & Continua, vol. 66, no. 1, pp. 183–216, 2021.
42. F. H. Riad, A. Radwan, E. M. Almetwally and M. Elgarhy, *A new heavy-tailed distribution with actuarial measures*, Journal of Radiation Research and Applied Sciences, vol. 16, no. 2, pp. 100562, 2023.
43. Z. Ahmad, E. Mahmoudi and S. Dey, *A new family of heavy-tailed distributions with an application to the heavy-tailed insurance loss data*, Communications in Statistics-Simulation and Computation, vol. 51, no. 8, pp. 4372–4395, 2022.
44. Z. Ahmad, E. Mahmoudi, M. Alizadeh, R. Roozegar and A. Z. Afify, *The Exponential T-X Family of Distributions: Properties and an Application to Insurance Data*, Journal of Mathematics, vol. 2021, no. 1, pp. 3058170, 2021.
45. W. A. Marambakuyana and S. C. Shongwe, *Composite and mixture distributions for heavy-tailed data—An application to insurance claims*, Mathematics, vol. 12, no. 2, pp. 335, 2024.
46. H. M. Aljohani, S. A. Bandar, H. Al-Mofleh, Z. Ahmad, M. El-Morshedy and A. Z. Afify, *A new asymmetric extended family: Properties and estimation methods with actuarial applications*, Plos one, vol. 17, no. 10, pp. e0275001, 2022.
47. P. Liu and Y. Zheng, *Heavy-tailed distributions of confirmed COVID-19 cases and deaths in spatiotemporal space*, Plos one, vol. 18, no. 11, pp. e0294445, 2023.
48. W. Zhao, S. K. Khosa, Z. Ahmad, M. Aslam and A. Z. Afify, *Type-I heavy-tailed family with applications in medicine, engineering and insurance*, Plos one, vol. 15, no. 8, pp. e0237462, 2020.